9-1-2012

Analysis and application of a free energy model for lens protein mixtures

Michael Bell

Analysis and Application of a Free Energy Model for Lens Protein Mixtures

by

Michael Bell

Submitted to the School of Mathematical Sciences

in partial fulfillment of the requirements for the degree of

Masters of Science

at the

ROCHESTER INSTITUTE OF TECHNOLOGY

September 2012

Author .....
Michael Bell
School of Mathematical Sciences

Accepted by .....
David S. Ross
School of Mathematical Sciences

Accepted by .....
George M. Thurston
Department of Physics

Accepted by .....
Christopher W. Wahle
School of Mathematical Sciences

Analysis and Application of a Free Energy Model for Lens Protein Mixtures

by

Michael Bell

Submitted to the School of Mathematical Sciences
on September 1, 2012, in partial fulfillment of the
requirements for the degree of
Masters of Science

Abstract

Cataract, the leading cause of blindness worldwide, has motivated a variety of investigations into the behavior of concentrated mixtures of eye lens proteins. While there has been success in modeling single protein solutions, a convenient model for mixtures is needed. We apply an analytically solvable sticky-hard sphere model to aqueous mixtures of alpha and gamma crystallin, two of the predominant proteins found in the mammalian eye lens. Developed by Baxter and Barboy, this model incorporates some of the fundamental characteristics of realistic mixtures, namely, variation in size and intermolecular attraction strength among each component. We show that light scattering intensities reconstructed from the model are in semi-quantitative agreement with experimental data. Our analysis of the model includes convenient algebraic reformulation for quantities used in light scattering expressions and using a parameter homotopy continuation method to solve a system of coupled quadratic equations arising in the model. Additionally, we derive analytic expressions for the second and third virial coefficients for the multicomponent sticky sphere potential, which describe the two and three body particle interactions, respectively.

Thesis Supervisor: David S. Ross, School of Mathematical Sciences
Thesis Supervisor: George M. Thurston, Department of Physics
Thesis Supervisor: Christopher W. Wahle, School of Mathematical Sciences

Contents

List of Figures

Chapter 1

Introduction

1.1 The Crystallin Lens and Cataract

Cataract, a condition affecting nearly 18 million people worldwide, is characterized by the opacification of the crystallin eye lens. As its name suggests, the primary function of the mammalian eye lens is to focus incoming light onto a photosensitive layer at the back of the eye called the retina. Incoming light stimulates photosensitive cells in the retina, converting them into electromagnetic impulses which travel to the brain via the optic nerve. The incident light rays must therefore pass unobstructed through the lens in order for a sharp image to be formed.

The crystallin lens is a transparent, biconvex structure containing thin, concentrically arranged cells called lens fibers. These fibers hold concentrated aqueous mixtures of three primary types of proteins: $\alpha-, \beta$ and $\gamma-$crystallins. The most common of these, α-crystallin, is a polydisperse multisubunit protein with a molecular weight ranging from 700,000 g/mol - 1,200,000 g/mol with a diameter of around 18 nm. β-crystallins come in two varieties with molecular weights ranging from 60,000 g/mol to 180,000 g/mol. Lastly, γ-crystallins are small, monomeric proteins with a molecular weight of approximately 20,000 g/mol and a diameter of around 4 nm. [2]. Figure 1-1 gives a size comparison of bovine α- and γ_B-crystallins, which are the primary focus of this thesis. This difference in protein size is one of the challenges in effectively modeling lens crystallin interactions.

Under normal conditions, these proteins are packed tightly in the lens fibers at concentrations exceeding 400 mg/ml in some regions of the lens. At such high concentrations, one would expect a large fraction of incoming light to be scattered before reaching the retina.

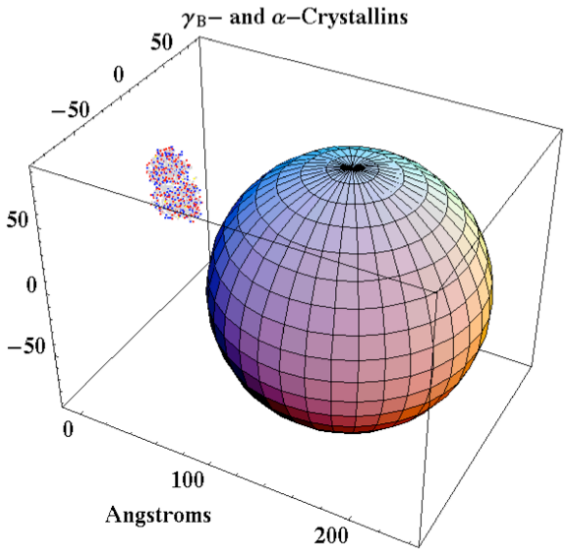

Figure 1-1: Size comparison of γ-crystallin (left) and α-crystallin (right)

However, it has been established that the liquid-like packing of the crystallins accounts for the transparency of the healthy lens [3] . This *short-range ordering* of the lens proteins minimizes fluctuations in protein density, which helps establish a uniform index of refraction, resulting in a clear image. Any disruption to this local uniformity in composition will result in increased lens turbidity and clouded vision. For this reason, cataract is classified together with Alzheimer's disease, sickle cell disease and others as a *protein condensation disease* [4]. These conditions are characterized by protein aggregation, condensation or separation which results in compromised cellular or organ functionality.

In order to design effective treatments for cataract, one must understand how the lens crystallins interact and how these interactions affect lens transparency. Previous studies have begun to quantify the interactions between proteins of the same species. It has been found that $\alpha - \alpha$ interactions can be modeled well by a hard sphere potential [5], and that γ_B-crystallin exhibit a short-range attraction to each other, which has been successfully modeled by a single component sticky-sphere model [6]. A convenient model for mixtures of different crystallin types is needed, and shall be the primary focus of this thesis.

1.2 Motivation and Goals

The motivation of this thesis stems from a series of observations demonstrating some interesting properties of mixtures of different crystallin types. Single point mutations in human

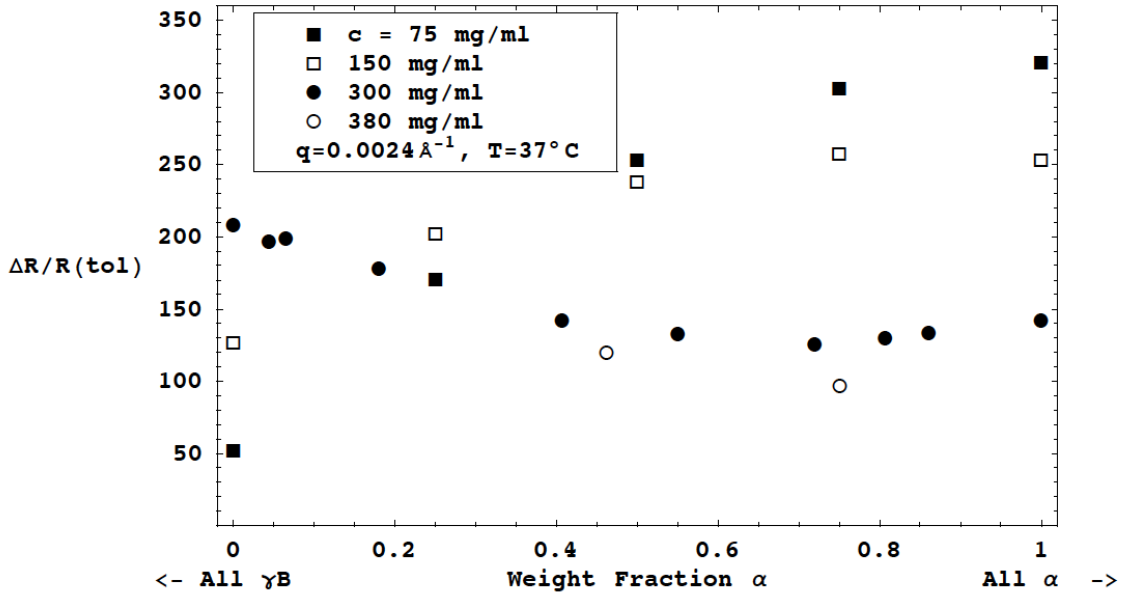

Figure 1-2: Light Scattering Intensity vs α-crystallin weight fraction for aqueous α/γ_B mixtures at 37° C at various total protein concentrations. At low concentrations (square markers) the light scattering intensity profile is concave down, while at high concentration (circular markers) the light scattering is concave up. Taken from [1] with permission.

γ-crystallin have been linked to congenital forms cataract simply by increasing the attraction strength between α and γ crystallins[7]. This finding is consistent with molecular dynamics simulations and thermodynamic perturbation theory [8, 9], which predicted the light scattering intensity and phase stability of bovine $\alpha - \gamma_B$ mixtures depends sensitively, and nonlinearly, on the $\alpha - \gamma$ interaction strength. Recent experiments [1] have shown the light scattering intensities of concentrated mixtures of bovine α and γ-crystallins are not simply a linear combination of the scattering of the constituent proteins. Furthermore, as seen in Fig (2-2), a qualitative change in the light scattering properties of these mixtures was observed as total protein volume fraction increased. At low total concentration (square markers), the light scattering profile is a concave down function of weight fraction α-crystallin, while at higher concentrations (circular markers) it is concave up. Our aim in this work is to reconstruct the light scattering intensities seen here using an analytically solvable statistical mechanical model.

In this thesis, we apply a multicomponent sticky-sphere liquid structure model, developed by Baxter and Barboy [10, 11], to reconstruct light scattering intensities for concentrated mixtures of α and γ_B. This model incorporates some of the key features of eye

lens protein mixtures, namely the differences in size and intermolecular interaction strength among the different types of lens crystallins. Despite being a highly idealized model, we have found that the calculated light scattering intensities are in good semi-quantitative agreement with experimental data, and capture many of the characteristics seen in the laboratory. Furthermore, we calculate analytic expressions for the second and third virial coefficients for the Baxter-Barboy model which can be useful in future experimental and theoretical investigations.

1.3 Outline

This thesis is organized in the following manner: In Chapter 2 we introduce the Baxter-Barboy multicomponent sticky-sphere model and discuss numerical schemes to solve an associated set of couple nonlinear equations. We introduce the fundamental light scattering equation and derive a convenient matrix factorization for the Hessian matrix of the Gibbs free energy for a two protein system, as predicted by the model. We compute light scattering intensities for concentrated aqueous $\alpha - \gamma_B$ crystallin mixtures and compare our results to experimental data. Chapter 4 is dedicated to deriving analytical expressions for the second and third virial coefficients for the Baxter-Barboy multicomponent potential. We end with a brief discussion and mention possible future work.

Chapter 2

The Baxter-Barboy Model

In this section we give a brief description of the multicomponent sticky-sphere model developed by Baxter and Barboy in the 1970s. We give an account of some of the mathematical manipulations we found convenient when using this model to reconstruct light scattering intensities for aqueous two-protein systems. This includes a numerical scheme to solve and select the physically meaningful roots of a system of coupled quadratic polynomials which define a set of model parameters. Using a compact expression for the Hessian of the Gibbs free energy, we compute light scattering efficiencies for aqeuous $\alpha - \gamma_B$ mixtures and compare with experiment.

2.1 Description of the Model

In the late 1960s, R. J. Baxter introduced a single component 'sticky-hard sphere' model of liquids [12] which incorporated some of the most fundamental features of realistic particle interactions: a potential that combined both intermolecular attraction and a repulsive 'hard-core'. This model generated much interest due to the fact that it was analytically solvable under the Percus-Yevick closure. Shortly afterward, Barboy [13] generalized Baxter's model to multicomponent mixtures of spheres of different sizes. As there has been success in using Baxter's original model for systems containing a single protein species [6], we attempt to apply Barboy's extension to multicomponent $\alpha - \gamma_B$ mixtures.

The Baxter-Barboy multicomponent model describes the interaction of M spherical molecules, each with respective diameter d_{ii} and number density $\rho_i = \frac{N_i}{V}$, $1 \leq i \leq M$. The

intermolecular potential, u_{ij}, between species i and j is defined by

$$e^{-u_{ij}(r)/k_BT} - 1 = \frac{d_{ij}}{2\tau_{ij}}\delta_-(d_{ij} - r) - H_-(d_{ij} - r) \tag{2.1.1}$$

where k_B is Boltzmann's constant, T is absolute temperature, $d_{ij} = \frac{1}{2}(d_{ii}+d_{jj})$ is the shortest center to center distance between a particle of species i and j. Additionally, τ_{ij} measures the attraction strength between species i and j and $\delta_-(x)$ and $H_-(x)$ are the asymmetric Dirac delta and asymmetric Heaviside step functions, respectively. The parameters τ_{ij} are generally temperature dependent and are defined so that $\tau_{ij} = 0$ represents infinitely strong adhesion between i and j and $\tau_{ij} \to \infty$ indicates hard-sphere behavior (no attraction) [11].

Barboy and Tenne [11] show that analytic expressions for the correlation functions, $c_{ij}(r)$, are attainable through the Percus-Yevick closure. These expressions are defined in terms of a set of dimensionless parameters, λ_{ij}, which are determined through the following system of coupled nonlinear polynomial equations:

$$\frac{\pi d_{ij}}{12(1-\xi_3)}\sum_k \rho_k d_{kk}^2(\lambda_{ik} - 6)(\lambda_{jk} - 6) - \tau_{ij}\lambda_{ij} = \frac{9d_{ij}\xi_2}{1-\xi_3} - \frac{d_{ij}^2}{d_{ii}d_{jj}} \tag{2.1.2}$$

where $1 \le i \le j \le M$ and $\xi_i = \sum \rho_k d_{kk}^i$. The quantities $\lambda_{ij} = \lambda_{ji}$, $\tau_{ij} = \tau_{ji}$ and $d_{ij} = d_{ji}$ are all invariant under permutation of their indices. Observe that through the Percus-Yevick closure, the task of determining $c_{ij}(r)$ has been turned from solving an integral equation to solving a system of algebraic equations.

2.2 Solving the Barboy-Tenne Equations

For an M component mixture, the system of quadratic equations in the λ_{ij} given in Eq. (2.1.2) generally has $M(M+1)$ complex solutions. However, we are only interested in *real* solutions to Eq. (2.1.2) and only a certain subset of these roots will have physical significance. Lahnovych [14] formulated the system in Eq. (2.1.2) as a matrix polynomial and examined the one- and two-component cases in detail. She also gave bounds on the τ_{ij} which guaranteed the existence of a real solution. In the present work, we derive a method to find the λ_{ij} in the specific two-component case of $\alpha - \gamma$ mixtures. We also discuss the general M-component case and describe a method for determining the physically relevant set of parameters, when real roots exist.

2.2.1 $\alpha - \gamma$ Mixtures

In the two-component case, the system given in Eq. (2.1.2) consists of the following three coupled quadratic equations in the unknowns $\lambda_{11}, \lambda_{12}$ and λ_{22}:

$$\frac{\pi}{12}\frac{d_{11}}{1-\xi_3}(\rho_1 d_{11}^2(\lambda_{11}-6)^2+\rho_2 d_{22}^2(\lambda_{12}-6)^2)-\tau_{11}\lambda_{11}=\frac{9d_{11}\xi_2}{1-\xi_3}-6 \tag{2.2.1}$$

$$\frac{\pi}{12}\frac{d_{12}}{1-\xi_3}(\rho_1 d_{11}^2(\lambda_{11}-6)(\lambda_{12}-6)+\rho_2 d_{22}^2(\lambda_{12}-6)(\lambda_{22}-6))-\tau_{12}\lambda_{12}=\frac{9d_{12}\xi_2}{1-\xi_3}-\frac{6d_{12}^2}{d_{11}d_{22}} \tag{2.2.2}$$

$$\frac{\pi}{12}\frac{d_{22}}{1-\xi_3}(\rho_1 d_{11}^2(\lambda_{12}-6)^2+\rho_2 d_{22}^2(\lambda_{22}-6)^2)-\tau_{22}\lambda_{22}=\frac{9d_{22}\xi_2}{1-\xi_3}-6 \tag{2.2.3}$$

It has been found that $\alpha-\alpha$ interactions can be accurately modeled as hard spheres [5]. In other words, we are interested in a two-component system for which $\tau_{22}\to\infty$. Two cases arise:

(1) $\lambda_{22}\to 0$ so that $\tau_{22}\lambda_{22}\to a$ for some constant a.

(2) $\lambda_{22}=c\tau_{22}$ and $\rho d_{22}^2(\lambda_{22}-6)2-\tau_{22}\lambda_{22}=0$.

In the first case, where $\lambda_{22}\to 0$, Eq. (2.2.3) becomes

$$\frac{\pi}{12}\frac{d_{22}}{1-\xi_3}(\rho_1 d_{11}^2(\lambda_{12}-6)^2+36\rho_2 d_{22}^2)-a=\frac{9d_{22}\xi_2}{1-\xi_3}-6 \tag{2.2.4}$$

which can always be satisfied for an appropriate choice of a. Thus, for $\lambda_{22}=0$ the system is reduced to

$$\frac{\pi}{12}\frac{d_{11}}{1-\xi_3}(\rho_1 d_{11}^2(\lambda_{11}-6)^2+\rho_2 d_{22}^2(\lambda_{12}-6)^2)-\tau_{11}\lambda_{11}=\frac{9d_{11}\xi_2}{1-\xi_3}-6 \tag{2.2.5}$$

$$\frac{\pi}{12}\frac{d_{12}}{1-\xi_3}(\rho_1 d_{11}^2(\lambda_{11}-6)(\lambda_{12}-6)-6\rho_2 d_{22}^2(\lambda_{12}-6))-\tau_{12}\lambda_{12}=\frac{9d_{12}\xi_2}{1-\xi_3}-\frac{6d_{12}^2}{d_{11}d_{22}} \tag{2.2.6}$$

To simplify calculation, we define $\phi_i=\frac{\pi}{6}\rho_i d_{ii}^3$, $x_i=\frac{\phi_i}{1-\xi_3}$, and $\gamma_{ij}=\frac{d_{ii}}{d_{jj}}$. In terms of these

new variables, (2.2.5) and (2.2.6) can be written

$$x_1(\lambda_{11}-6)^2+\gamma_{ij}x_2(\lambda_{12}-6)^2-2\tau_{11}(\lambda_{11}-6)=12\tau_{11}+18(x_1+\gamma_{ij}x_2)-12 \quad (2.2.7)$$

$$(\lambda_{12}-6)\left[(1+\gamma_{ij})(x_1(\lambda_{11}-6)-6\gamma_{ij}x_2)-4\gamma_{ij}\tau_{12}\right]$$
$$=18(1+\gamma_{ij})(x_1+\gamma_{ij}x_2)-6(1+\gamma_{ij})^2+24\gamma_{ij}\tau_{12} \quad (2.2.8)$$

Solving Eq (2.2.8) for $(\lambda_{12}-6)$ we obtain

$$(\lambda_{12}-6)=\frac{18(x_1+\gamma_{ij}x_2)-6(1+\gamma_{ij})+\frac{24\gamma_{ij}\tau_{12}}{1+\gamma_{ij}}}{x_1(\lambda_{11}-6)-6\gamma_{ij}x_2)-\frac{4\gamma_{ij}\tau_{12}}{1+\gamma_{ij}}}. \quad (2.2.9)$$

Writing

$$A=18(x_1+\gamma_{ij}x_2)-6(1+\gamma_{ij})+\frac{24\gamma_{ij}\tau_{12}}{1+\gamma_{ij}} \quad (2.2.10)$$

$$B=-6\gamma_{ij}x_2)-\frac{4\gamma_{ij}\tau_{12}}{1+\gamma_{ij}} \quad (2.2.11)$$

$$C=12\tau_{11}+18(x_1+\gamma_{ij}x_2)-12 \quad (2.2.12)$$

and substituting Eq. (2.2.9) into Eq. (2.2.7) yields

$$x_1(\lambda_{11}-6)^2+\gamma_{ij}x_2\frac{A^2}{[x_1(\lambda_{11}-6)+B]^2}-2\tau_{11}(\lambda_{11}-6)=C. \quad (2.2.13)$$

Upon multiplying Eq. (2.2.13) by $\frac{[x_1(\lambda_{11}-6)+B]^2}{x_1^3}$ and collecting coefficients we get

$$(\lambda_{11}-6)^4+D_3(\lambda_{11}-6)^3+D_2(\lambda_{11}-6)^2+D_1(\lambda_{11}-6)+D_0=0 \quad (2.2.14)$$

where

$$D_3=\frac{2Bx_1^2-2x_1^2\tau_{11}}{x_1^3}$$
$$D_2=\frac{x_1B^2-4B\tau_{11}x_1-Cx_1^2}{x_1^3}$$
$$D_1=\frac{-2B^2\tau_{11}-2BCx_1}{x_1^3}$$
$$D_0=\frac{A^2\gamma_{ij}x_2-CB^2}{x_1^3}.$$

which is a fourth order monic polynomial in $(\lambda_{11} - 6)$. Observe that knowledge of λ_{11} leads to λ_{12} through Eq. (2.2.9) so we have transformed the task of solving Eqs. (2.2.5) - (2.2.6) into solving a single fourth order polynomial. The roots of (2.2.14) can be found numerically by using an eigenvalue routine on the matrix

$$M = \begin{bmatrix} 0 & 1 & 0 & 0 \\ 0 & 0 & 1 & 0 \\ 0 & 0 & 0 & 1 \\ -D_0 & -D_1 & -D_2 & -D_3 \end{bmatrix}$$

which has characteristic polynomial $x^4 + D_3x^3 + D_2x^2 + D_1x + D_0$.

2.2.2 General Case

In the general M-component case, for which no assumptions on the τ_{ij} are made, it is not as straightforward to reduce Eq. (2.1.2) to a simpler algebraic equation. In principle, we could solve Eqs. (2.1.2) by simply applying a numerical scheme such as Newton-Raphson. However, even with knowledge of initial guesses that would converge to all solutions to this system, we would require external selection critera in order to choose the correct physical root. In light of this, we apply a method from numerical algebraic geometry known as Parameter Homotopy Continuation [15, 16]. The basic idea is we begin with a system for which we have (approximate) knowlege of the physical root. We continuously transform this system into the target system of interest, by embedding it in a *homotopy* and tracking the roots of the changing system. At the end of this transformation, we expect to have a solution to the target system corresponding to the known solution.

Consider a polynomial system, $\mathbf{f}(\lambda, \boldsymbol{\tau}) = \mathbf{0}$ where

$$\mathbf{f}(\lambda, \boldsymbol{\tau}) = \begin{bmatrix} f_1(\lambda, \tau) \\ f_2(\lambda, \tau) \\ \vdots \\ f_M(\lambda, \tau)) \end{bmatrix} \tag{2.2.15}$$

is a vector of M polynomials in the M unknowns $\lambda = (\lambda_1, \ldots, \lambda_M)$ and $\boldsymbol{\tau}$ is a set of parameters which appear as coefficients in the f_i. Suppose we are able to find the solution

λ_0 when $\boldsymbol{\tau} = \boldsymbol{\tau}_0$ and wish to find solution λ_1 when $\boldsymbol{\tau} = \boldsymbol{\tau}_1$. To do this, we embed the *start system* $\mathbf{f}(\lambda, \boldsymbol{\tau}_0)$ and the *target system*, $\mathbf{f}(\lambda, \boldsymbol{\tau}_1)$, in the *coefficient-parameter homotopy*

$$\mathbf{h}(\lambda, t) = \mathbf{f}(\lambda, (1-t)\boldsymbol{\tau}_0 + t\boldsymbol{\tau}_1) = \mathbf{0}, \qquad t \in [0, 1] \tag{2.2.16}$$

Observe that as t goes from 0 to 1, $h(\lambda, t)$ is continuously deformed from the initial system $\mathbf{h}(\lambda, 0) = \mathbf{f}(\lambda, \boldsymbol{\tau}_0)$ to the target system $\mathbf{h}(\lambda, 1) = \mathbf{f}(\lambda, \boldsymbol{\tau}_1)$.

Since the roots of polynomial equations depend continuously on their coefficients, we may then follow the path the known solution λ_0 takes as t goes from 0 to 1. To accomplish this, we employ a *secant predictor-corrector* method in which, at each iteration, we increment t to $t_{n+1} = t_n + \delta$ and *predict* the solution to the equation

$$\mathbf{h}(\lambda_{n+1}, t_n + \delta) = \mathbf{0} \tag{2.2.17}$$

using the secant predictor

$$\lambda_{n+1} \approx \lambda_n + \delta(\lambda_n - \lambda_{n-1}). \tag{2.2.18}$$

This approximate solution then serves as the initial guess for a Newton-Raphson method which *corrects* our prediction to find the true value of λ_{n+1}, solving Eq. (2.2.17). In order to ensure convergence, we adapt the step size δ based on the success or failure of the corrector step.

It is known that for systems of hard sphere particles, or for $\{\tau_{ij}\} \to \infty$, all the $\{\lambda_{ij}\}$ will vanish [13]. Thus, if we start the homotopy continuation method, Eq. (2.2.16), at large values of the τ_{ij}, say $\boldsymbol{\tau_0} = \tau_{\mathbf{max}}$ we should expect the solution, $\boldsymbol{\lambda_0}$, of the start system to be approximately $\mathbf{0}$. This now gives us a way to identify the set of physically significant roots at τ_0 and to track using the previously described method to the target values of the τ_{ij} given in $\tau_\mathbf{1}$. In practice, this has proven to be an extremely reliable method for solving Eq. (2.1.2) in both the two and three component cases.

2.3 Light Scattering Equation

One of the main sources of light scattering in the eye lens is caused by spatial variations of the refractive index due to local fluctuations in protein composition. For particles suspended in

a solvent, the amount of scattered light is usually represented by a quantity called the excess Rayleigh ratio, $\Delta R(\theta)$. The excess Rayleigh ratio describes the intensity of the scattered light in excess of that of pure solvent at a scattering angle θ. Kirkwood and Goldberg [17] have shown that the near forward ($\theta = 0$) excess rayleigh ratio for fluid mixtures is given by

$$\Delta R(0) = \left(\frac{\pi^2 k_B T}{\lambda^4}\right) \nabla_\rho \varepsilon^T \cdot H_\rho[G/V]^{-1} \cdot \nabla_\rho \varepsilon \tag{2.3.1}$$

where k_B is Boltzmann's constant, T is absolute temperature, λ is the wavelength of incident light, $\nabla_\rho \varepsilon$ is the gradient of the dielectric coefficient, ε, with respect to number density, ρ. The quantity $H_\rho[G/V]^{-1}$ is the inverse of the Hessian matrix of the Gibbs free energy per unit volume with respect to number density which is defined as

$$H_\rho[G/V] = \begin{bmatrix} \frac{\partial^2 \frac{G}{V}}{\partial \rho_1^2} & \frac{\partial^2 \frac{G}{V}}{\partial \rho_1 \partial \rho_2} \\ \frac{\partial^2 \frac{G}{V}}{\partial \rho_1 \partial \rho_2} & \frac{\partial^2 \frac{G}{V}}{\partial \rho_2^2} \end{bmatrix}. \tag{2.3.2}$$

The quantity of fundamental importance in Eq. (2.3.1) is the Gibbs free energy G, along its functional dependence on composition (specifically, its second partial derivatives). The liquid structure model we have chosen to analyze $\alpha - \gamma_B$ mixtures will lead us to an analytical expression for these quantities, from which we can reconstruct light scattering intensities. In the next section, we derive a convenient matrix factorization for $H_\rho[G/V]$ for systems containing two solutes in solution.

2.4 Free Energy of Two-Solute mixtures

Our primary goal is to reconstruct light scattering intensities for aqueous α/γ-crystallin mixtures, which is a three-component system. While we could consider the solvent as a third species in a three component system, the McMillan-Mayer theory of solutions [18] allows us to treat solvent effects implicitly in a two component system. In the latter system, the solvent is assumed to be a continuum which fills the remaining volume between the solute particles.

We must determine the correspondence between the thermodynamic properties of the explicit three component system and the implicit two component system. If we let chemical species 0 be the solvent, the relationship between the two component chemical potential

$\mu_i^{(2)}$ and the three component chemical potential $\mu_i^{(3)}$ of species $i = 1, 2$ can be shown to be

$$\mu_i^{(2)} = \mu_i^{(3)} - \frac{\overline{v}_i}{\overline{v}_0}\mu_0^{(3)} \tag{2.4.1}$$

where $\overline{v}_j$ is the partial molecular volume of component j. From Eq. (A5) in [19] we have

$$\mu_0/\overline{v}_0 = g + \left(\frac{\partial g}{\partial \rho_1}\right)(-\rho_1) + \left(\frac{\partial g}{\partial \rho_2}\right)(-\rho_2) \tag{2.4.2}$$

where $g = G/V$ is the Gibbs free energy per unit volume. Differentiating Eq. (2.4.1) for $i = 1, 2$ with respect to $\rho_j (j = 1, 2)$ and using Eq. (2.4.2), we obtain

$$\begin{bmatrix} \frac{\partial \mu_1^{(2)}}{\partial \rho_1} & \frac{\partial \mu_1^{(2)}}{\partial \rho_2} \\ \frac{\partial \mu_2^{(2)}}{\partial \rho_1} & \frac{\partial \mu_2^{(2)}}{\partial \rho_2} \end{bmatrix} = \begin{bmatrix} \frac{\partial \mu_1^{(3)}}{\partial \rho_1} & \frac{\partial \mu_1^{(3)}}{\partial \rho_2} \\ \frac{\partial \mu_2^{(3)}}{\partial \rho_1} & \frac{\partial \mu_2^{(3)}}{\partial \rho_2} \end{bmatrix} + \begin{bmatrix} \overline{v}_1\rho_1 & \overline{v}_1\rho_2 \\ \overline{v}_2\rho_1 & \overline{v}_2\rho_2 \end{bmatrix} H_\rho[g] \tag{2.4.3}$$

where

$$H_\rho[g] = \begin{bmatrix} \frac{\partial^2 g}{\partial \rho_1^2} & \frac{\partial^2 g}{\partial \rho_1 \rho_2} \\ \frac{\partial^2 g}{\partial \rho_1 \rho_2} & \frac{\partial^2 g}{\partial \rho_2^2} \end{bmatrix} \tag{2.4.4}$$

is the Hessian of the intensive Gibbs free energy with respect to number densities. It is also shown in [19] that the matrix of partial derivatives of the 3-component chemical potentials with respect to ρ_1 and ρ_2 is related to $H_\rho[g]$ by

$$\begin{bmatrix} \frac{\partial \mu_1^{(3)}}{\partial \rho_1} & \frac{\partial \mu_1^{(3)}}{\partial \rho_2} \\ \frac{\partial \mu_2^{(3)}}{\partial \rho_1} & \frac{\partial \mu_2^{(2)}}{\partial \rho_2} \end{bmatrix} = \begin{bmatrix} 1 - \rho_1\overline{v}_1 & -\rho_2\overline{v}_1 \\ -\rho_1\overline{v}_2 & 1 - \rho_2\overline{v}_2 \end{bmatrix} H_\rho[g] \tag{2.4.5}$$

Substituting Eq. (2.4.5) into Eq. (2.4.3) yields

$$H_\rho \begin{bmatrix} G \\ \overline{V} \end{bmatrix} = \begin{bmatrix} \frac{\partial \mu_1^{(2)}}{\partial \rho_1} & \frac{\partial \mu_1^{(2)}}{\partial \rho_2} \\ \frac{\partial \mu_2^{(2)}}{\partial \rho_1} & \frac{\partial \mu_2^{(2)}}{\partial \rho_2} \end{bmatrix}. \tag{2.4.6}$$

Thus the Hessian of the intensive Gibbs free energy of the experimental system is equal to the matrix of partial derivatives of the two-component chemical potentials. For solutions modeled by the Baxter-Barboy mutlicomponent model these derivatives are shown to be

$$\frac{\partial \mu_i}{\partial \rho_j} = \frac{1}{\beta}(\rho_i\rho_j)^{-1/2} \sum_k Q_{ki}Q_{kj} \tag{2.4.7}$$

where $\beta = 1/k_B T$ where k is Boltzmann's constant, T is absolute temperature and the Q_{ij} are functions of the set of parameters $\{\lambda_{ij}\}$ [11].

2.4.1 Matrix Factorization of $H_\rho\left[\frac{G}{V}\right]$

We shall now derive a convenient matrix factorization for $H_\rho\left[\frac{G}{V}\right]$ in which the Q_{ij} appearing in Eq. (2.4.7) are considered to be the ij entry of the matrix $\mathbf{Q}$ defined as

$$\mathbf{Q} = \sqrt{\boldsymbol{\rho}}\boldsymbol{X}^{-1}(\boldsymbol{I} + \boldsymbol{X}\boldsymbol{L} \circ \boldsymbol{\gamma})(\boldsymbol{I} + \boldsymbol{X}\boldsymbol{U})\boldsymbol{X}\sqrt{\boldsymbol{\rho}}^{-1} \tag{2.4.8}$$

where $A \circ B$ is the Schur product defined by $(A \circ B)_{ij} = A_{ij}B_{ij}$ and

$$\boldsymbol{\rho} = \begin{bmatrix} \rho_1 & & \\ & \rho_2 & \\ & & \ddots \end{bmatrix} \quad \boldsymbol{X} = \begin{bmatrix} x_1 & & \\ & x_2 & \\ & & \ddots \end{bmatrix} \quad \boldsymbol{L} = \begin{bmatrix} l_{11} & l_{12} & \cdots \\ l_{12} & l_{22} & \cdots \\ \vdots & \vdots & \ddots \end{bmatrix} \tag{2.4.9}$$

$$\boldsymbol{\gamma} = \begin{bmatrix} 1 & \frac{d_{11}}{d_{22}} & \\ \frac{d_{22}}{d_{11}} & 1 & \\ & & \ddots \end{bmatrix} \qquad \boldsymbol{U} = \begin{bmatrix} 1 & 1 & \cdots \\ 1 & 1 & \cdots \\ \vdots & \vdots & \ddots \end{bmatrix}. \tag{2.4.10}$$

In the above equations, ρ_i and d_{ii} are the number density and diameter of species i, respectively, $x_i = \frac{\phi_i}{1-\sum_k \phi_k}$ where ϕ_i is the volume fraction of species i and $l_{ij} = 3 - \lambda_{ij}$.

The quantities Q_{ij} are defined in Eq. (52) of [11] as

$$Q_{ij} = \delta_{ij} - 2\pi(\rho_i\rho_j)^{1/2}\int_{m_{ij}}^{d_{ij}} q_{ij}(r)dr \tag{2.4.11}$$

where

$$d_{ij} = \frac{1}{2}(d_{ii} + d_{jj}) \tag{2.4.12}$$

$$m_{ij} = \frac{1}{2}(d_{ii} - d_{jj}) \tag{2.4.13}$$

$$q_{ij}(r) = \left[\frac{1}{2}a_i(r^2 - d_{ij}^2) + b_i(r - d_{ij}) + t_{ij}\right] H_-(d_{ij} - r) \tag{2.4.14}$$

$$a_i = \frac{1}{(1-\xi_3)^2}\left(1 - \xi_3 + 3\xi_2 d_{ii} - \frac{\pi}{6} d_{ii} \sum_k \rho_k d_{kk}^2 \lambda_{ik}\right) \tag{2.4.15}$$

$$b_i = \frac{1}{2} d_{ii}\left(\frac{1}{1-\xi_3} - a_i\right) \tag{2.4.16}$$

$$\xi_i = \frac{\pi}{6} \sum_k \rho_k d_{kk}^i \tag{2.4.17}$$

$$t_{ij} = \frac{\lambda_{ij} d_{ii} d_{jj}}{12(1-\xi_3)} \tag{2.4.18}$$

Substituting these quantities into Eq. (2.4.11) and integrating we obtain

$$Q_{ij} = \delta_{ij} - 2\pi(\rho_i\rho_j)^{1/2} \int_{m_{ij}}^{d_{ij}} \left[\frac{1}{2}a_i(r^2 - d_{ij}^2) + b_i(r - d_{ij}) + t_{ij}\right] dr \tag{2.4.19}$$

$$= \delta_{ij} - 2\pi(\rho_i\rho_j)^{1/2} \int_{m_{ij}}^{d_{ij}} \left[\frac{a_i}{2}r^2 + b_i r + \left(t_{ij} - b_i d_{ij} - \frac{d_{ij}^2 a_i}{2}\right)\right] dr \tag{2.4.20}$$

$$= \delta_{ij} - 2\pi(\rho_i\rho_j)^{1/2} \left[\frac{a_i}{6}r^3 + \frac{b_i}{2}r^2 + \left(t_{ij} - b_i d_{ij} - \frac{d_{ij}^2 a_i}{2}\right) r\right]_{\frac{1}{2}(d_{ii}-d_{jj})}^{\frac{1}{2}(d_{ii}+d_{jj})} \tag{2.4.21}$$

$$= \delta_{ij} - 2\pi(\rho_i\rho_j)^{1/2} \left[\frac{a_i}{24}(3d_{ii}^2 d_{jj} + d_{jj}^3) + \frac{b_i}{2}d_{ii}d_{jj} + \left(t_{ij} - b_i d_{ij} - \frac{d_{ij}^2 a_i}{2}\right) d_{jj}\right] \tag{2.4.22}$$

$$= \delta_{ij} - 2\pi(\rho_i\rho_j)^{1/2} \Big[\frac{a_i}{24}(3d_{ii}^2 d_{jj} + d_{jj}^3) + \frac{d_{ii}^2 d_{jj}}{4}\left(\frac{1}{1-\xi_3} - a_i\right) + \left(t_{ij} - \frac{d_{ii}d_{ij}}{2}\left(\frac{1}{1-\xi_3} - a_i\right) - \frac{d_{ij}^2 a_i}{2}\right) d_{jj}\Big] \tag{2.4.23}$$

$$= \delta_{ij} - 2\pi(\rho_i\rho_j)^{1/2} \Big[a_i\left(\frac{3d_{ii}^2 d_{jj} + d_{jj}^3}{24} - \frac{d_{ii}^2 d_{jj}}{4} + \frac{d_{ii}d_{ij}d_{jj}}{2} - \frac{d_{ij}^2 d_{jj}}{2}\right) + \frac{d_{ii}^2 d_{jj}}{4(1-\xi_3)} - \frac{d_{ii}d_{ij}d_{jj}}{2(1-\xi_3)} + d_{jj}t_{ij}\Big] \tag{2.4.24}$$

$$= \delta_{ij} - 2\pi(\rho_i\rho_j)^{1/2} \left[-a_i\frac{d_{jj}^3}{12} + \frac{d_{ii}^2 d_{jj}}{4(1-\xi_3)} - \frac{d_{ii}d_{ij}d_{jj}}{2(1-\xi_3)} + \frac{\lambda_{ij}d_{ii}d_{jj}^2}{12(1-\xi_3)}\right] \tag{2.4.25}$$

$$= \delta_{ij} - 2\pi(\rho_i\rho_j)^{1/2} \left[-a_i\frac{d_{jj}^3}{12} + \frac{1}{1-\xi_3}\left(\frac{d_{ii}d_{jj}}{12}\lambda_{ij} - \frac{d_{ii}d_{jj}^2}{4}\right)\right] \tag{2.4.26}$$

$$= \delta_{ij} + 2\pi(\rho_i\rho_j)^{1/2} \left[a_i\frac{d_{jj}^3}{12} + \frac{1}{12(1-\xi_3)}\left(3d_{ii}d_{jj}^2 - d_{ii}d_{jj}^2\lambda_{ij}\right)\right] \tag{2.4.27}$$

$$= \delta_{ij} + \frac{\pi}{6}\sqrt{\frac{\rho_i}{\rho_j}} \cdot \rho_j \left[a_i d_{jj}^3 + \frac{d_{ii}d_{jj}^2}{(1-\xi_3)}\left(3 - \lambda_{ij}\right)\right] \tag{2.4.28}$$

Observe that if we define $x_k = \frac{\pi}{6}\rho_k d_{kk}^3$, $\gamma_{ij} = \frac{d_{ii}}{d_{jj}}$ and $l_{ij} = 3 - \lambda_{ij}$ then a_i can be rewritten

as

$$a_i = \frac{1}{(1-\xi_3)^2}\left(1-\xi_3+3\xi_2 d_{ii}-\frac{\pi}{6}d_{ii}\sum_k \rho_k d_{kk}^2\lambda_{ik}\right) \tag{2.4.29}$$

$$= \frac{1}{(1-\xi_3)^2}\left(1-\xi_3+3\frac{\pi}{6}\sum_k \rho_k d_{kk}^2 d_{ii}-\frac{\pi}{6}d_{ii}\sum_k \rho_k d_{kk}^2\lambda_{ik}\right) \tag{2.4.30}$$

$$= \frac{1}{(1-\xi_3)^2}\left(1-\xi_3+3\frac{\pi}{6}\sum_k \rho_k d_{kk}^3\frac{d_{ii}}{d_{kk}}-\frac{\pi}{6}\sum_k \rho_k d_{kk}^3\frac{d_{ii}}{d_{kk}}\lambda_{ik}\right) \tag{2.4.31}$$

$$= \frac{1}{1-\xi_3}\left(1+3\frac{\pi}{6}\sum_k \frac{\rho_k d_{kk}^3}{1-\xi_3}\gamma_{ik}-\frac{\pi}{6}\sum_k \frac{\rho_k d_{kk}^3}{1-\xi_3}\gamma_{ik}\lambda_{ik}\right) \tag{2.4.32}$$

$$= \frac{1}{1-\xi_3}\left(1+3\sum_k x_k\gamma_{ik}-\sum_k x_k\gamma_{ik}\lambda_{ik}\right) \tag{2.4.33}$$

$$= \frac{1}{1-\xi_3}\left(1+\sum_k x_k\gamma_{ik}(3-\lambda_{ik})\right) \tag{2.4.34}$$

which upon substitution in Eq. (2.4.28) yeilds

$$Q_{ij} = \delta_{ij}+\frac{\pi}{6}\sqrt{\frac{\rho_i}{\rho_j}}\cdot\rho_j\left[\frac{d_{jj}^3}{1-\xi_3}\left(1+\sum_k x_k\gamma_{ik}(3-\lambda_{ik})\right)+\frac{d_{ii}d_{jj}^2}{(1-\xi_3)}(3-\lambda_{ij})\right] \tag{2.4.35}$$

$$= \delta_{ij}+\sqrt{\frac{\rho_i}{\rho_j}}\cdot\left[\frac{\frac{\pi}{6}\rho_j d_{jj}^3}{1-\xi_3}\left(1+\sum_k x_k\gamma_{ik}(3-\lambda_{ik})\right)+\frac{\frac{\pi}{6}\rho_j d_{jj}^3\gamma_{ij}}{(1-\xi_3)}(3-\lambda_{ij})\right] \tag{2.4.36}$$

$$= \delta_{ij}+\sqrt{\frac{\rho_i}{\rho_j}}\cdot\left[x_j\left(1+\sum_k x_k\gamma_{ik}(3-\lambda_{ik})\right)+x_j\gamma_{ij}(3-\lambda_{ij})\right] \tag{2.4.37}$$

$$= \delta_{ij}+\sqrt{\frac{\rho_i}{\rho_j}}\cdot\left[x_j\left(1+\sum_k x_k\gamma_{ik}l_{ik}\right)+x_j\gamma_{ij}l_{ij}\right] \tag{2.4.38}$$

$$= \delta_{ij}+x_j\sqrt{\frac{\rho_i}{\rho_j}}\cdot\left[\left(1+\gamma_{ij}l_{ij}+\sum_k x_k\gamma_{ik}l_{ik}\right)\right]. \tag{2.4.39}$$

We see that the diagonal elements, Q_{ii}, have the form

$$Q_{ii} = 1+x_i+x_i l_{ii}+x_i\sum_k x_k\gamma_{ik}l_{ik} \tag{2.4.40}$$

and the off diagonal elements are

$$Q_{ij} = x_j\sqrt{\frac{\rho_i}{\rho_j}}\left[1+\gamma_{ij}l_{ij}+\sum_k x_k\gamma_{ik}l_{ik}\right] \tag{2.4.41}$$

which is consistent with the factorization given in Eq. (2.4.8). Using the matrix entry formulation for the Q_{ij} together with Eq. (2.4.7) gives the factorization

$$H_\rho\left[\frac{G}{V}\right] = \begin{bmatrix} \frac{\partial^2 g}{\partial \rho_1^2} & \frac{\partial^2 g}{\partial \rho_1 \rho_2} \\ \frac{\partial^2 g}{\partial \rho_1 \rho_2} & \frac{\partial^2 g}{\partial \rho_2^2} \end{bmatrix} = \frac{1}{\beta}\sqrt{\boldsymbol{\rho}}^{-1}\boldsymbol{Q}^{\mathrm{T}}\boldsymbol{Q}\sqrt{\boldsymbol{\rho}}^{-1}. \tag{2.4.42}$$

The expression for ΔR given in Eq. (2.3.1) involves the *inverse* of $H_\rho\left[G/V\right]$ which we see is simply

$$H_\rho\left[\frac{G}{V}\right]^{-1} = \beta\sqrt{\boldsymbol{\rho}}\boldsymbol{Q}^{-1}(\boldsymbol{Q}^{-1})^{\mathrm{T}}\sqrt{\boldsymbol{\rho}}. \tag{2.4.43}$$

Substituting Eq. (2.4.43) into Eq. (2.3.1) yields

$$\Delta R(0) = \left(\frac{\pi^2}{\lambda^4}\right)\nabla_\rho \varepsilon^T \cdot \sqrt{\boldsymbol{\rho}}\boldsymbol{Q}^{-1}(\boldsymbol{Q}^{-1})^{\mathrm{T}}\sqrt{\boldsymbol{\rho}} \cdot \nabla_\rho \varepsilon. \tag{2.4.44}$$

While Eq. (2.4.44) gives an expression for ΔR in terms of the model parameters, it is will be more convenient to express $\nabla_\rho \varepsilon$ in terms of changes in the index of refraction, n, with respect to protein mass per unit volume concentrations. The concentration of species i is related to the number density, ρ_i, by

$$c_i = \rho_i m_i \tag{2.4.45}$$

where m_i is the mass per particle of species i. Using the relation $\varepsilon = n^2$ we find that

$$\frac{\partial \varepsilon}{\partial \rho_i} = m_i \frac{\partial n^2}{\partial c_i} \tag{2.4.46}$$

$$= 2nm_i \frac{\partial n}{\partial c_i} \tag{2.4.47}$$

which gives

$$\nabla_\rho \epsilon^{\mathrm{T}} = 2n\left(m_1\frac{\partial n}{\partial c_1}, m_2\frac{\partial n}{\partial c_2}\right). \tag{2.4.48}$$

This is desirable as experimental measurements for $\frac{\partial n}{\partial c}$ are available for α and γ_B-crystallin. Using Eq. (2.4.48), the final form for the light scattering intensity for a two-solute ternary mixture is

$$\Delta R(0) = \left(\frac{4n^2\pi^2}{\lambda^4}\right)\left(m_1\frac{\partial n}{\partial c_1}, m_2\frac{\partial n}{\partial c_2}\right) \cdot \sqrt{\boldsymbol{\rho}}\boldsymbol{Q}^{-1}(\boldsymbol{Q}^{-1})^{\mathrm{T}}\sqrt{\boldsymbol{\rho}} \cdot \left(m_1\frac{\partial n}{\partial c_1}, m_2\frac{\partial n}{\partial c_2}\right)^{\mathrm{T}}. \tag{2.4.49}$$

We are now in a position to compare light scattering intensities as predicted by the Baxter-Barboy model with those obtained via experiment.

2.5 Reconstructed Light Scattering for $\alpha - \gamma_B$ mixtures

We use the above development to construct light scattering intensity vs. concentration plots for mixtures of bovine α and γ_B-crystallin in water using $\lambda = 514$ nm light. We choose particle diameters $d_{\gamma\gamma} = 1.8$ nm and $d_{\alpha\alpha} = 7.55$ nm. Based on previous work mentioned earlier, the $\alpha - \alpha$ interactions as hard spheres, $\tau_{\alpha\alpha} = \infty$. Fine [6] derived the following temperature dependence for the $\gamma - \gamma$ attraction:

$$\tau_{\gamma\gamma}(T) = 0.012T + 0.55 \tag{2.5.1}$$

For molecular weights, we take $M_\gamma = 20,981$ g/mol and $M_\alpha = 750,000$ g/mol. We model the index of refraction as a function of mass/volume concentrations c_γ and c_α using

$$n = n_0 + \frac{\partial n}{\partial c_\gamma} c_\gamma + \frac{\partial n}{\partial c_\alpha} c_\alpha \tag{2.5.2}$$

where we take $n_0 = 1.33$ and $\frac{\partial n}{\partial c_\gamma} = 0.21$, $\frac{\partial n}{\partial c_\alpha} = 0.17$. Using these parameters in computational software such as MATLAB or Mathematica, we run over the $\alpha - \gamma_B$ concentration grid and solve Eqs. (2.1.2) for $\{\lambda_{ij}\}$. We can then compute $\Delta R(0)$ via Eq. (2.4.49).

We present some preliminary results, using the parameters listed above, which demonstrate the ability for the sticky-sphere model to reproduce many of the key features seen in light scattering experiments. Figures (2-1), (2-2) and (2-3) show light scattering intensity vs concentration plots for aqueous $\alpha - \gamma_B$ crystallin, reconstructed using the Baxter-Barboy sticky-sphere model at 37° C, 25° C and 15° C, respectively. Here, we have taken $\tau_{\alpha\gamma} = 7$. The filled circles are experimental data as measured by Thurston [1] and are organized by total protein concentration. From Fig. (2-1), we see that the sticky-sphere model is able to reproduce the change in concavity in the light scattering intensity observed when moving from low concentration (blue points) to high concentration (red points). The model also accurately reproduces the variation in light scattering intensity at 300 mg/ml, as a function of temperature as seen across Figs (2-1)-(2-3).

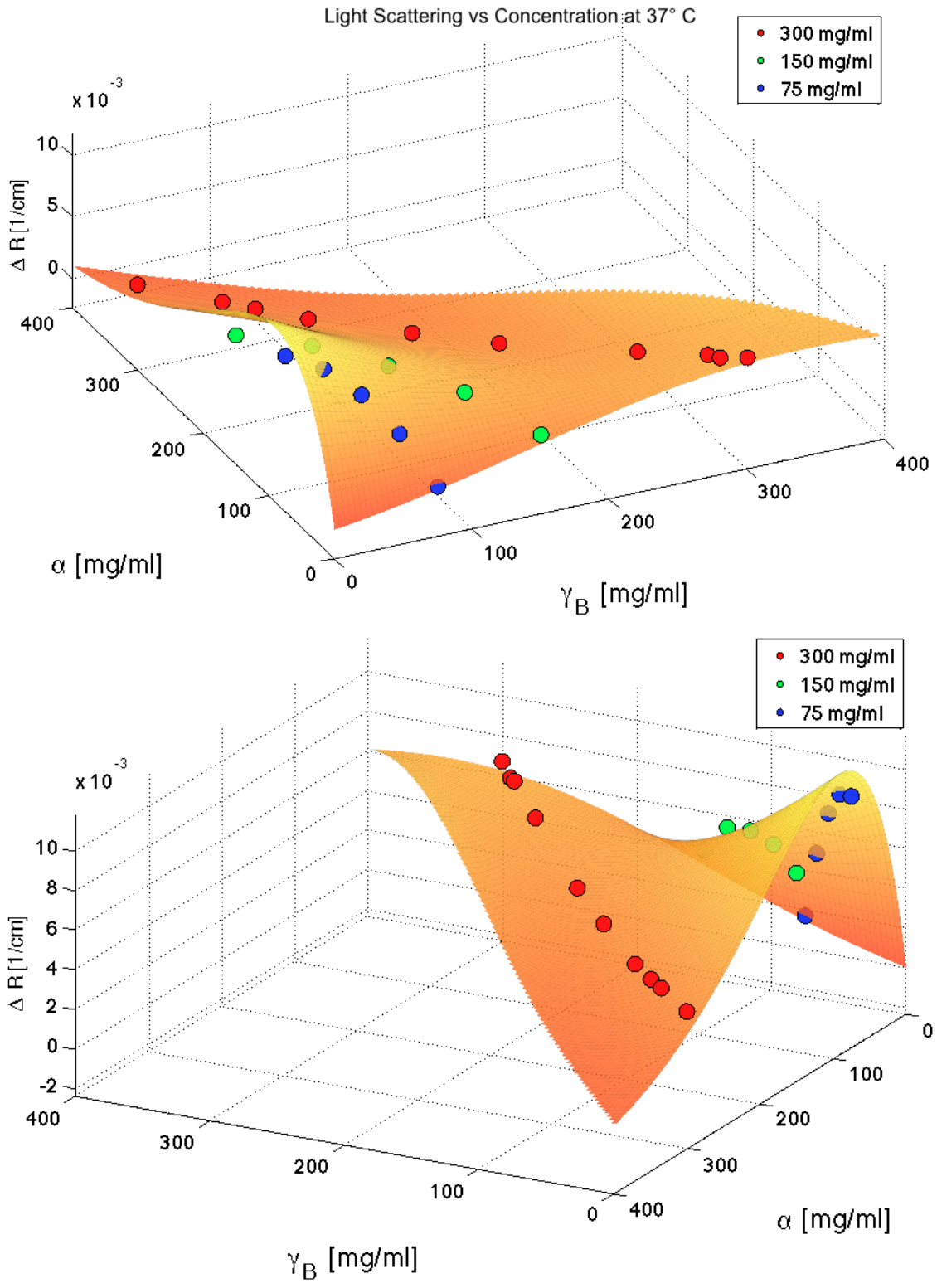

Figure 2-1: Reconstructed Light Scattering Intensity vs Concentration plots for $\alpha - \gamma_B$ mixtures at 37° C, using model parameters described in the text and $\tau_{\alpha\gamma} = 7$. The filled circles are experimental data measurements corresponding to 300 mg/ml (red), 150 mg/ml (green) and 75 mg/ml (blue) total protein concentration.

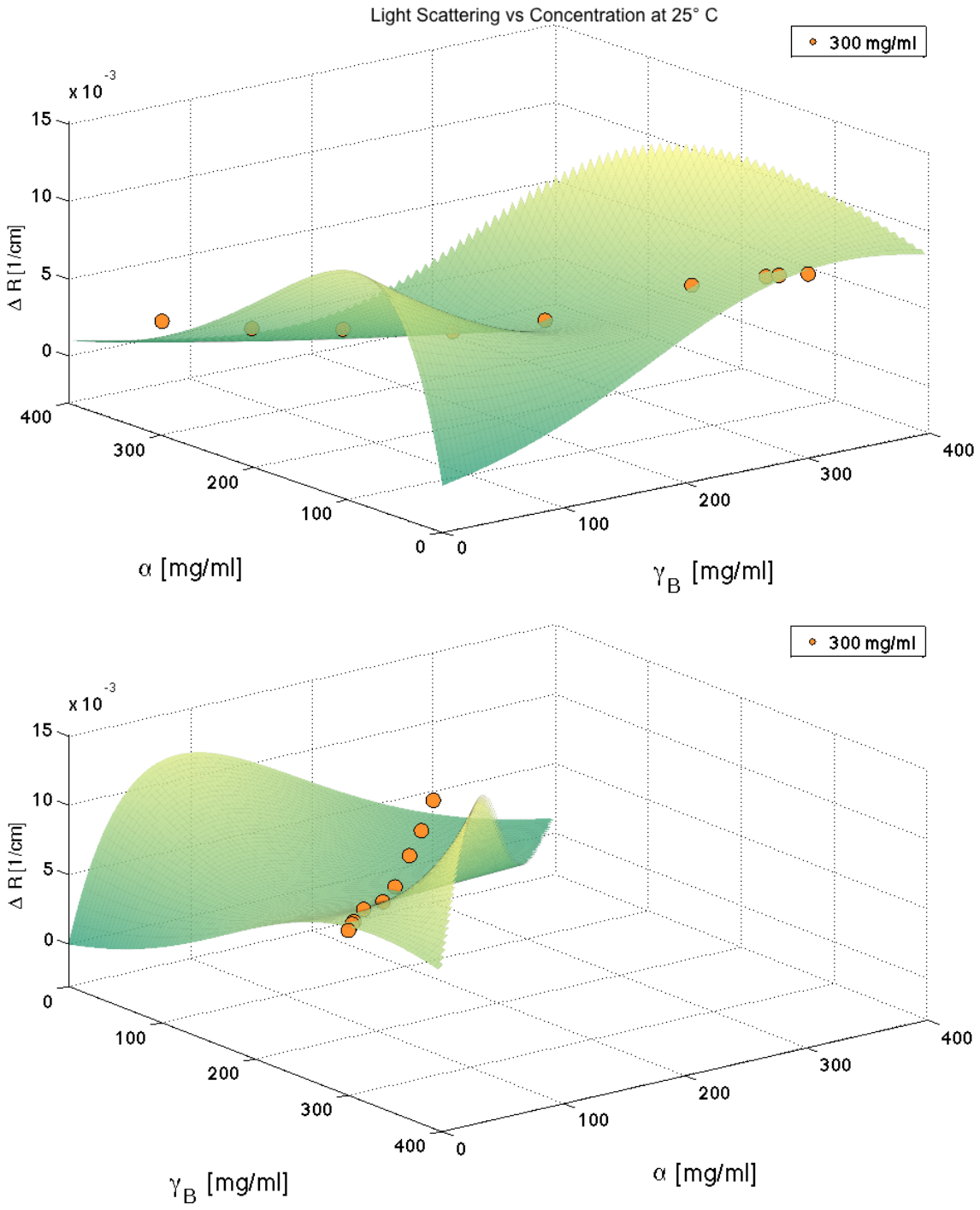

Figure 2-2: Reconstructed Light Scattering Intensity vs Concentration plots for $\alpha - \gamma_B$ mixtures at 25° C, using model parameters described in the text and $\tau_{\alpha\gamma} = 7$. The filled circles are experimental data measurements corresponding to 300 mg/ml (orange) total protein concentration.

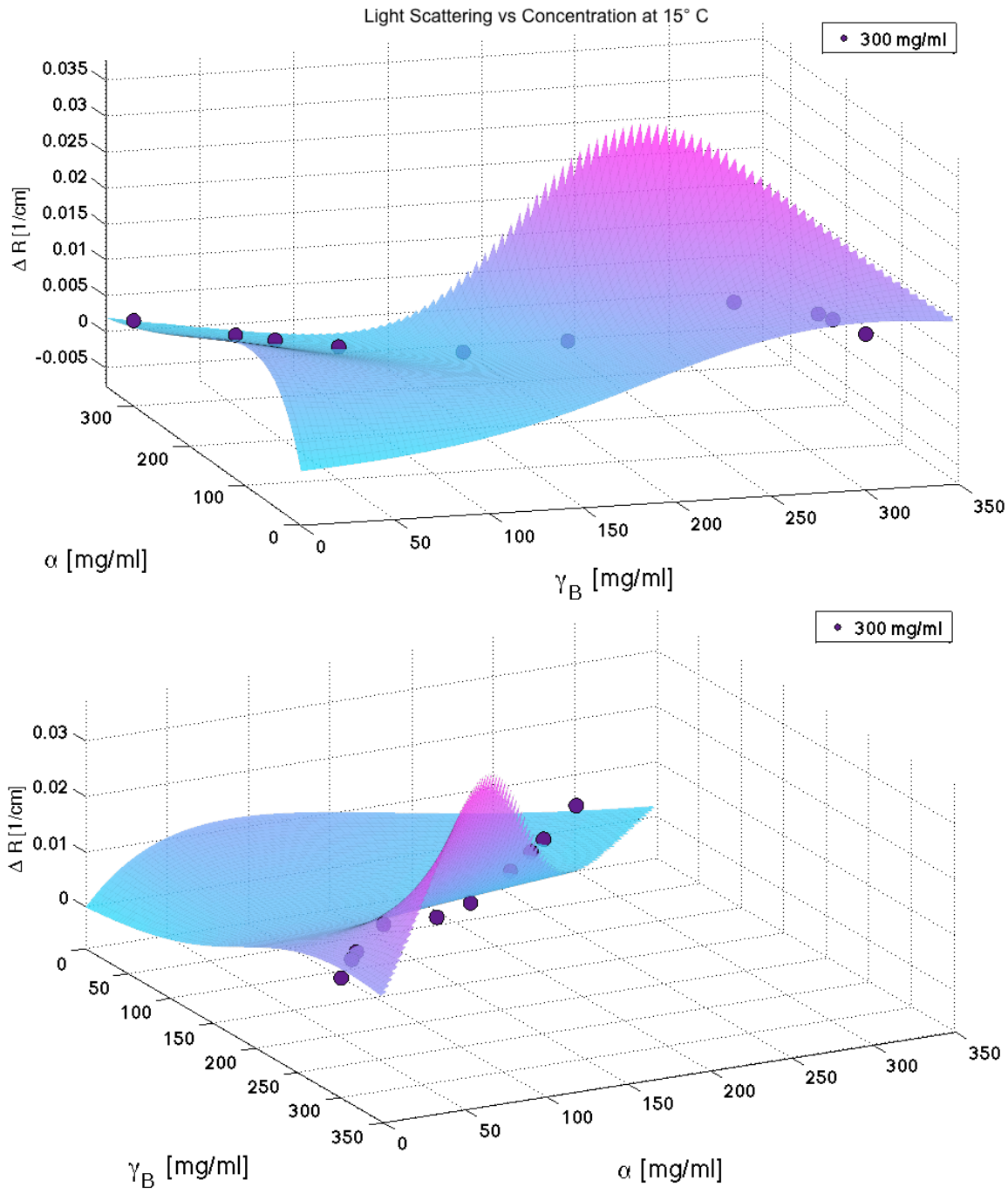

Figure 2-3: Reconstructed Light Scattering Intensity vs Concentration plots for $\alpha - \gamma_B$ mixtures at 15° C, using model parameters described in the text and $\tau_{\alpha\gamma} = 7$. The filled circles are experimental data measurements corresponding to 300 mg/ml (purple) total protein concentration.

Chapter 3

Virial Coefficients

We now shift our attention to calculating the virial coefficients for the Baxter-Barboy potential. We are able to derive closed-form expressions for both the second and third virial coefficients for this model, using some clever techniques of integration. These expressions can offer theoretical insight into the light scattering behavior seen in the previous section. Additionally, virial coefficients may be measured experimentally and can be useful in determining the nature of crystallin interactions.

3.1 Introduction

The pressure of a single component system can be expressed as an infinite power series in the number density ρ

$$\frac{P}{k_B T} = \rho + B_2(T)\rho^2 + B_3(T)\rho^3 + \dots \tag{3.1.1}$$

Eq. (3.1.1) is known as the *virial equation of state* and is a modification of the ideal gas law which corrects for the interaction of particles in real systems. The coefficients $B_n(T)$, known as the n^{th} virial coefficient, arises directly from the interaction forces between n particles. This clear interpretation, together with the fact that they can be measured experimentally, make virial coefficients an extremely important tool in understanding the behavior of gases and liquids.

The expansion given in Eq. (3.1.1) can be generalized for a system with M components

$$\frac{P}{k_B T} = \sum_{i=1}^{M} \rho_i + \sum_{i=1}^{M}\sum_{j=1}^{M} B_{ij}\rho_i\rho_j + \sum_{i=1}^{M}\sum_{j=1}^{M}\sum_{k=1}^{M} C_{ijk}\rho_i\rho_j\rho_k + \dots \tag{3.1.2}$$

where ρ_i is the number density of species i and B_{ij}, $C_{ijk}, \ldots$ are the second, third, etc. mixture virial coefficients and depend on temperature. The second virial coefficient, B_{ij}, depends on two particle interactions between species i and j, the third virial coefficient ,C_{ijk}, depends on three particle interactions between species i, j and k, and so on. Note that the virial coefficients are invariant under permutation of the indices, so $B_{ij} = B_{ji}$, $C_{ijk} = C_{jki} = C_{ikj}$, etc.

In addition to the pressure, other thermodynamic quantities can be expressed as a virial expansion in the number densities. In particular, the excess Gibbs free energy per unit volume per k_BT for a two component system may be written [20]

$$\frac{G}{Vk_BT} = \rho_1 \ln \rho_1 + \rho_2 \ln \rho_2 + B_{11}\rho_1^2 + 2B_{12}\rho_1\rho_2 + B_{22}\rho_2^2 + \frac{C_{111}\rho_1^3 + 3C_{112}\rho_1^2\rho_2 + 3C_{122}\rho_1\rho_2^2 + C_{222}\rho_2^3}{2} + \ldots \tag{3.1.3}$$

Knowledge of the virial coefficients makes it possible to calculate light scattering intensities using Eq. (3.1.3). This may lead to additional insight into lens transparency, as the virial coefficients depend only on the form of the intermolecular potential and not on the Percus-Yevick closed used in solving the Baxter-Barboy model.

The second virial coefficients $B_{ij}(T)$ are the easiest to compute and depend only on the pairwise potential $u_{ij}(r)$ between a particle of type i and j. In order to calculate the third virial coefficient $C_{ijk}(T)$ one generally requires knowledge of the *total* three body interaction potential. However, if one assumes *pairwise additivity* of intermolecular forces, the task of computing higher order virial coefficients is greatly simplified. Pairwise additivity assumes multibody effects are negligible and the total intermolecular potential of a group of molecules can be written as the sum of their pairwise potentials. For example, assuming pairwise additivity, the total intermolecular interaction, U_{ijk} between particles i, j and k can be written

$$U_{ijk}(\vec{r}_i, \vec{r}_j, \vec{r}_k) = u_{ij}(|\vec{r}_i - \vec{r}_j|) + u_{jk}(|\vec{r}_j - \vec{r}_k|) + u_{ik}(|\vec{r}_i - \vec{r}_k|) \tag{3.1.4}$$

where $\vec{r}_i, \vec{r}_j$ and $\vec{r}_k$ are the positions of particles i, j and k, respectively [21, 22]. Under this assumption, we are able to derive analytic expressions for B_{ij} and C_{ijk} for the Baxter-Barboy potential.

3.2 Second Virial Coefficient for the Baxter-Barboy Potential

The second virial coefficients $B_{ij}(T)$ are given by

$$B_{ij}(T) = -2\pi \int_0^\infty f_{ij}(r) r^2 dr \tag{3.2.1}$$

where $u_{ij}(r)$ is the pairwise intermolecular potential between species i and j and

$$f_{ij}(r) = e^{-u_{ij}(r)/k_B T} - 1 \tag{3.2.2}$$

is called the Mayer f-function [21].

In the Baxter-Barboy sticky-hard sphere model, the Mayer f-function for interactions between species i and j is given by

$$f_{ij}(r) = \left(\frac{d_{ij}}{2\tau_{ij}}\right) \delta_-(d_{ij} - r) + H_-(r - d_{ij}). \tag{3.2.3}$$

Here, $d_{ij} = \frac{1}{2}(d_{ii} + d_{jj})$ is the smallest center-to-center distance between species i and j, τ_{ij} is a temperature dependent measure of the strength of intermolecular attraction and $\delta_-(x)$ and $H_-(x)$ are the asymmetric Dirac delta function and asymmetric Heaviside step function, respectively.

By Eq. (3.2.1) and Eq. (3.2.3) we obtain

$$B_{ij}(T) = -2\pi \int_0^\infty \left[\left(\frac{d_{ij}}{2\tau_{ij}}\right) \delta_-(d_{ij} - r) + H_-(r - d_{ij}) - 1\right] r^2 dr \tag{3.2.4}$$

$$= -2\pi \int_0^{d_{ij}} \left[\left(\frac{d_{ij} r^2}{2\tau_{ij}}\right) \delta_-(d_{ij} - r) - r^2\right] r^2 dr \tag{3.2.5}$$

$$= \frac{2\pi}{3} d_{ij}^3 \left(1 - \frac{3}{2\tau_{ij}}\right) \tag{3.2.6}$$

where the temperature dependence arises through the parameter τ_{ij}.

3.3 Third Virial Coefficient for the Baxter-Barboy Potential

Under the assumption of pairwise additivity of intermolecular forces, the third virial coefficient is given by

$$C_{ijk}(T) = -\frac{1}{3}\int\int f_{ij}(|\boldsymbol{r}_{ij}|)f_{jk}(|\boldsymbol{r}_{jk}|)f_{ik}(|\boldsymbol{r}_{ik}|)d\boldsymbol{r}_{ij}d\boldsymbol{r}_{ik} \tag{3.3.1}$$

where $\boldsymbol{r}_{ab} = \boldsymbol{r}_b - \boldsymbol{r}_a$, and f_{ij} is the Mayer f-function defined in Eq. (3.2.2). Using the properties of Fourier transforms, it can be shown that the integral in Eq. (3.3.1) can be written

$$C_{ijk}(T) = -\frac{4\pi(2\pi)^{3/2}}{3}\int_0^\infty \gamma_{ij}(t)\gamma_{jk}(t)\gamma_{ik}(t)t^2\,dt \tag{3.3.2}$$

where $\gamma_{\alpha\gamma}(t)$ is the Fourier transform of $f_{\alpha\gamma}(|\boldsymbol{r}|)$ [21, 22] . Taking the Fourier transform of the mayer f-function given in Eq. (3.2.3) we obtain

$$\gamma_{\alpha\gamma}(t) = \frac{1}{(2\pi)^{3/2}}\int f_{\alpha\gamma}(|\boldsymbol{r}|)e^{-i\boldsymbol{t}\cdot\boldsymbol{r}}d\boldsymbol{r} \tag{3.3.3}$$

$$= \left(\frac{2}{\pi}\right)^{1/2}\int_0^\infty f_{\alpha\gamma}(r)\frac{r\sin tr}{t}dr \tag{3.3.4}$$

$$= \left(\frac{2}{\pi}\right)^{1/2}\int_0^{d_{\alpha\gamma}}\left[\left(\frac{d_{\alpha\gamma}}{2\tau_{\alpha\gamma}}\right)\delta_-(d_{\alpha\gamma}-r) + H_-(r-d_{\alpha\gamma}) - 1\right]\frac{r\sin tr}{t}dr \tag{3.3.5}$$

$$= \left(\frac{2}{\pi}\right)^{1/2}\left[\frac{d_{\alpha\gamma}^2\sin d_{\alpha\gamma}t}{2\tau_{\alpha\gamma}t} + \frac{d_{\alpha\gamma}\cos d_{\alpha\gamma}t}{t^2} - \frac{\sin d_{\alpha\gamma}t}{t^3}\right] \tag{3.3.6}$$

$$= \left(\frac{2}{\pi}\right)^{1/2} d_{\alpha\gamma}^3\left[\frac{\sin d_{\alpha\gamma}t}{2d_{\alpha\gamma}\tau_{\alpha\gamma}t} + \frac{\cos d_{\alpha\gamma}t}{(d_{\alpha\gamma}t)^2} - \frac{\sin d_{\alpha\gamma}t}{(d_{\alpha\gamma}t)^3}\right] \tag{3.3.7}$$

Eq. (3.3.2) becomes

$$\begin{aligned} &C_{ijk}(T) \\ &= -\frac{32\pi}{3}d_{ij}^3d_{jk}^3d_{ik}^3\int_0^\infty\left[\frac{\sin d_{ij}t}{2d_{ij}\tau_{ij}t} + \frac{\cos d_{ij}t}{(d_{ij}t)^2} - \frac{\sin d_{ij}t}{(d_{ij}t)^3}\right]\left[\frac{\sin d_{jk}t}{2d_{jk}\tau_{jk}t} + \frac{\cos d_{jk}t}{(d_{jk}t)^2} - \frac{\sin d_{jk}t}{(d_{jk}t)^3}\right]\times \\ &\qquad\left[\frac{\sin d_{ik}t}{2d_{ik}\tau_{ik}t} + \frac{\cos d_{ik}t}{(d_{ik}t)^2} - \frac{\sin d_{ik}t}{(d_{ik}t)^3}\right]t^2dt \end{aligned} \tag{3.3.8}$$

The integral appearing in Eq. (3.3.8) is of the form

$$I = I(A,B,C,\tau_A,\tau_B,\tau_C) = \int_0^\infty\left[\frac{\sin At}{2A\tau_At} + g(At)\right]\left[\frac{\sin Bt}{2B\tau_Bt} + g(Bt)\right]\left[\frac{\sin Ct}{2C\tau_Ct} + g(Ct)\right]t^2dt \tag{3.3.9}$$

where $A = \frac{1}{2}(d_{ii} + d_{jj})$, $B = \frac{1}{2}(d_{jj} + d_{kk})$, $C = \frac{1}{2}(d_{ii} + d_{kk})$, τ_A, τ_B, τ_C are positive, real parameters and

$$g(x) = \frac{\cos x}{x^2} - \frac{\sin x}{x^3}. \tag{3.3.10}$$

We note that each bracketed expression in the integrand of Eq. (3.3.9) is an even function of t, and therefore

$$I = \frac{1}{2}\int_{-\infty}^{\infty} \left[\frac{\sin At}{2A\tau_A t} + g(At)\right]\left[\frac{\sin Bt}{2B\tau_B t} + g(Bt)\right]\left[\frac{\sin Ct}{2C\tau_C t} + g(Ct)\right] t^2 dt. \tag{3.3.11}$$

Expanding the integrand of Eq. (3.3.11) yields

$$\begin{aligned} I = \frac{1}{2}\int_{-\infty}^{\infty} \Big[&\frac{\sin At \sin Bt \sin Ct}{8\tau_A\tau_B\tau_C ABCt} + \frac{\sin At \sin Bt}{4\tau_A\tau_B AB} g(Ct) + \frac{\sin At \sin Ct}{4\tau_A\tau_C AC} g(Bt) \\ &+ \frac{\sin Bt \sin Ct}{4\tau_B\tau_C BC} g(At) + \frac{\sin At}{2\tau_A A} g(Bt)g(Ct)t + \frac{\sin Bt}{2\tau_B Bt} g(At)g(Ct)t \\ &+ \frac{\sin Ct}{2\tau_C Ct} g(At)g(Bt)t + g(At)g(Bt)g(Ct)t^2\Big] dt \end{aligned} \tag{3.3.12}$$

Splitting up the integral in Eq. (3.3.12) results in integrals of four distinct types, namely

$$T_1(A,B,C) = \int_{-\infty}^{\infty} \frac{\sin At \ \sin Bt \ \sin Ct}{t} dt \tag{3.3.13}$$

$$T_2(A,B,C) = \int_{-\infty}^{\infty} \sin At \ \sin Bt \ g(Ct) dt \tag{3.3.14}$$

$$T_3(A,B,C) = \int_{-\infty}^{\infty} \sin At \ g(Bt) \ g(Ct) t dt \tag{3.3.15}$$

$$T_4(A,B,C) = \int_{-\infty}^{\infty} g(At) \ g(Bt) \ g(Ct) t^2 dt \tag{3.3.16}$$

each of which can be evaluated in closed form.

The following two lemmas will be useful:

Lemma 3.3.1 (Riemann-Lebesgue Lemma) *Let f be a L^1 integrable function. Then*

$$\lim_{\lambda\to\infty} \int_{-\infty}^{\infty} f(x)\sin(\lambda x)\, dx = 0$$

and

$$\lim_{\lambda\to\infty}\int_{-\infty}^{\infty} f(x)\cos(\lambda x)\,dx = 0$$

Lemma 3.3.2 *Let f be a continuous, L^1 integrable function. Then*

$$\lim_{\lambda\to\infty}\int_{-\infty}^{\infty}\frac{\sin(\lambda x)}{x}f(x)\,dx = \lim_{x\to 0} f(x)\pi.$$

Proofs of Lemmas (3.3.1)-(3.3.2) can be found in [23] and [24], respectively. Additionally, we define

$$\begin{aligned}Y_n(A,B,C) = \frac{\pi}{4n!}\big[&(A+B+C)^{n-1}|A+B+C| + (A-B-C)^{n-1}|A-B-C| + \\ &(-1)^n(-A+B-C)^{n-1}|-A+B-C| + (-1)^n(-A-B+C)^{n-1}|-A-B+C|\big]\end{aligned} \tag{3.3.17}$$

for nonnegative integers, n, and note that

$$\frac{\partial Y_n(A,B,C)}{\partial A} = Y_{n-1}(A,B,C). \tag{3.3.18}$$

3.3.1 Type I Integral

To evaluate integrals of the first type, we note that by expressing $\sin x$ in terms of complex exponentials, we can derive the identity

$$\begin{aligned}\sin At\ \sin Bt\ \sin Ct = -\frac{1}{4}\big[&\sin(A+B+C)t + \sin(A-B-C)t + \\ &\sin(-A+B-C)t + \sin(-A-B+C)t\big]\end{aligned} \tag{3.3.19}$$

Thus, Eq. (3.3.13) becomes

$$T_1 = -\frac{1}{4}\int_{-\infty}^{\infty}\frac{\sin(A+B+C)t}{t} + \frac{\sin(A-B-C)t}{t} + \frac{\sin(-A+B-C)t}{t} + \frac{\sin(-A-B+C)t}{t}dt. \tag{3.3.20}$$

Using the well known result

$$\int_{-\infty}^{\infty}\frac{\sin\sigma t}{t}dt = \mathrm{sgn}(\sigma)\cdot\pi \tag{3.3.21}$$

a proof of which can be found in [25], we find

$$T_1(A,B,C) = -\frac{\pi}{4}\Big[\mathrm{sgn}(A+B+C) + \mathrm{sgn}(A-B-C) + \mathrm{sgn}(-A+B-C) + \mathrm{sgn}(-A-B+C)\Big] \tag{3.3.22}$$

In light of the fact that we can write $\mathrm{sgn}(x) = \dfrac{x}{|x|}$, for non-zero x, we obtain

$$T_1(A,B,C) = -Y_0(A,B,C). \tag{3.3.23}$$

We shall demonstrate that in the physical context of the problem, the quantities $A-B-C, -A-B+C$ and $-A+B-C$ are never zero, and are in fact strictly negative. We will therefore assume that the family of functions $Y_n(A,B,C)$ are continuous for all physically admissable values of A, B and C.

3.3.2 Type II Integrals

We begin by observing that

$$g(\beta t) = \frac{1}{\beta t^2}\frac{\partial}{\partial \beta}\left(\frac{\sin \beta t}{\beta t}\right). \tag{3.3.24}$$

Thus, the integral of the second type, given by Eq. (3.3.14), can be written

$$T_2(A,B,C) = \frac{1}{C}\frac{\partial}{\partial C}\frac{1}{C}\int_{-\infty}^{\infty}\frac{\sin At \sin Bt \sin Ct}{t^3}\,dt. \tag{3.3.25}$$

where we have interchanged the order of integration and differentiation. If we now define

$$I_3(A,B,C) = \int_{-\infty}^{\infty}\frac{\sin At \sin Bt \sin Ct}{t^3}dt \tag{3.3.26}$$

differentiating Eq. (3.3.26) twice with respect to the parameter A yields

$$\frac{\partial I_3(A,B,C)}{\partial A} = \int_{-\infty}^{\infty}\frac{\cos At \sin Bt \sin Ct}{t^2}dt \tag{3.3.27}$$

and

$$\frac{\partial^2 I_3(A,B,C)}{\partial A^2} = -\int_{-\infty}^{\infty} \frac{\sin At \sin Bt \sin Ct}{t} dt \tag{3.3.28}$$

$$= -T_1(A,B,C) \tag{3.3.29}$$

From Eq. (3.3.23) we obtain

$$\frac{\partial^2 I_3(A,B,C)}{\partial A^2} = Y_0(A,B,C) \tag{3.3.30}$$

Integrating both sides of Eq. (3.3.30) with respect to A yields

$$\frac{\partial I_3}{\partial A} = Y_1(A,B,C) + \eta_1(B,C) \tag{3.3.31}$$

where η_1 is arbitrary function of B and C. Equating the right sides of Eq. (3.3.30) and Eq. (3.3.31), we obtain

$$\int_{-\infty}^{\infty} \frac{\cos At \sin Bt \sin Ct}{t^2} dt = Y_1(A,B,C) + \eta_1(B,C) \tag{3.3.32}$$

By Lemma 3.3.1 the left hand side of Eq. (3.3.32) must vanish as $A \to \infty$. Taking the same limit of the right hand side of Eq. (3.3.32), we find

$$\lim_{A\to\infty} -\frac{\pi}{4}\left[|A+B+C| + |A-B-C| - |-A+B-C| - |-A-B+C|\right] + \eta_1(B,C)$$

$$= \eta_1(B,C) \tag{3.3.33}$$

since $Y_1(A,B,C)$ vanishes for $A > B + C$. Since these limits must be equal, we must have $\eta_1(B,C) \equiv 0$, which gives

$$\frac{\partial I_3}{\partial A} = Y_1(A,B,C) \tag{3.3.34}$$

and thus

$$I_3(A,B,C) = Y_2(A,B,C) + \eta_2(B,C). \tag{3.3.35}$$

If we take the limit as $A \to \infty$ of Eq. (3.3.26) and apply Lemma 3.3.2 we obtain

$$\begin{aligned}\lim_{A\to\infty} I_3(A,B,C) &= \lim_{A_\infty} \int_{-\infty}^{\infty} \frac{\sin At}{t} \cdot \frac{\sin Bt \sin Ct}{t^2} dt \\ &= \pi \lim_{t\to 0} \left[\frac{\sin Bt \sin Ct}{t^2} \right] \\ &= \pi BC \end{aligned} \tag{3.3.36}$$

Taking the same limit of Eq. (3.3.35) we find

$$\begin{aligned}\lim_{A\to\infty} I_3(A,B,C) = \lim_{A\to\infty} \frac{\pi}{8} \Big[&(A+B+C)^2 + (A-B-C)^2 - \\ &(-A+B-C)^2 - (-A-B+C)^2 \Big] + \eta_2(B,C) \\ = \lim_{A\to\infty} \frac{\pi}{8} &\left[2(B+C)^2 - 2(B-C)^2 \right] + \eta_2(B,C) \\ = \pi BC &+ \eta_2(B,C) \end{aligned} \tag{3.3.37}$$

which, by Eq. (3.3.36) gives $\eta_2 \equiv 0$ and so

$$I_3(A,B,C) = Y_2(A,B,C) \tag{3.3.38}$$

and

$$T_2(A,B,C) = \frac{1}{C} \frac{\partial}{\partial C} \frac{Y_2(A,B,C)}{C} \tag{3.3.39}$$

3.3.3 Type III Integrals

Using Eq. (3.3.24) one can write

$$T_3(A,B,C) = \frac{1}{BC}\frac{\partial}{\partial C}\frac{\partial}{\partial B}\int_{-\infty}^{\infty}\frac{\sin At\sin Bt\sin Ct}{BCt^5}dt \tag{3.3.40}$$

We observe that the integral in Eq. (3.3.40) does not converge. However, we may add a regularization term inside the integrand which does not depend on B, as the derivative with respect to B will cause these terms to vanish. Specifically, we have

$$T_3(A,B,C) = \frac{1}{BC}\frac{\partial}{\partial C}\frac{\partial}{\partial B}\int_{-\infty}^{\infty}\frac{\sin At\sin Bt\sin Ct}{BCt^5} - \frac{\sin At\sin t\sin Ct}{Ct^5}dt \tag{3.3.41}$$

$$= \frac{1}{BC}\frac{\partial}{\partial C}\frac{\partial}{\partial B}\int_{-\infty}^{\infty}\frac{\sin At}{t}\left[\frac{\sin Bt}{Bt^3} - \frac{\sin t}{t^3}\right]\frac{\sin Ct}{Ct}dt \tag{3.3.42}$$

If we let

$$I_5(A,B,C) = \int_{-\infty}^{\infty}\frac{\sin At}{t}\left[\frac{\sin Bt}{Bt^3} - \frac{\sin t}{t^3}\right]\frac{\sin Ct}{Ct}dt \tag{3.3.43}$$

then,

$$\frac{\partial I_5}{\partial A} = \int_{-\infty}^{\infty}\cos At\left[\frac{\sin Bt}{Bt^3} - \frac{\sin t}{t^3}\right]\frac{\sin Ct}{Ct}dt \tag{3.3.44}$$

$$\frac{\partial^2 I_5}{\partial A^2} = -\int_{-\infty}^{\infty}\sin At\left[\frac{\sin Bt}{Bt^3} - \frac{\sin t}{t^3}\right]\frac{\sin Ct}{C}\,dt \tag{3.3.45}$$

Expanding the integrand in Eq. (3.3.45) we find

$$\frac{\partial^2 I_5}{\partial A^2} = -\int_{-\infty}^{\infty}\frac{\sin At\sin Bt\sin Ct}{BCt^3} - \frac{\sin At\sin t\sin Ct}{Ct^3}dt \tag{3.3.46}$$

$$= -\frac{1}{BC}I_3(A,B,C) + \frac{1}{C}I_3(A,1,C) \tag{3.3.47}$$

$$= -\frac{1}{BC}Y_2(A,B,C) + \frac{1}{C}Y_2(A,1,C) \tag{3.3.48}$$

where we have used the result obtained in Eq. (3.3.38). Integrating, we find

$$\frac{\partial I_5}{\partial A} = -\frac{1}{BC}Y_3(A,B,C) + \frac{1}{C}Y_3(A,1,C) + \eta_1(B,C) \tag{3.3.49}$$

$$I_5 = -\frac{1}{BC}Y_4(A,B,C) + \frac{1}{C}Y_4(A,1,C) + A\eta_1(B,C) + \eta_2(B,C) \tag{3.3.50}$$

where η_1 and η_2 are arbitrary functions of integration, which we will again determine by

comparing the limits of Eqs. (3.3.43 - 3.3.44) to Eqs. (3.3.49 - 3.3.50) as $A \to \infty$.

We begin by noting that the function $h(t) = \left[\frac{\sin Bt}{Bt^3} - \frac{\sin t}{t^3}\right] \frac{\sin Ct}{Ct}$ is bounded, smooth and integrable (prove this?) and hence by Lemma 3.3.1

$$\lim_{A\to\infty} \frac{\partial I_5}{\partial A} = 0 \tag{3.3.51}$$

and by Lemma 3.3.2

$$\lim_{A\to\infty} I_5 = \pi \lim_{t\to 0} \left[\frac{\sin Bt}{Bt^3} - \frac{\sin t}{t^3}\right] \frac{\sin Ct}{Ct} \tag{3.3.52}$$

$$= \pi \lim_{t\to 0} \left[\left(\frac{Bt}{Bt3} - \frac{(Bt)^3}{3!Bt^3} + \frac{(Bt)^5}{5!Bt^3} + \dots\right) - \left(\frac{t}{t3} - \frac{(t)^3}{3!t^3} + \frac{(t)^5}{5!t^3} + \dots\right)\right] \frac{\sin Ct}{t} \tag{3.3.53}$$

$$= \frac{\pi}{6}(1 - B^2) \tag{3.3.54}$$

Furthermore, taking the limit as $A \to \infty$ of Eq. (3.3.49) yields

$$\lim_{A\to\infty} \frac{\partial I_5}{\partial A} = \lim_{A\to\infty} -\frac{\pi}{24BC}\left[(A+B+C)^3 + (A-B-C)^3 + (-A+B-C)^3 + (-A-B+C)^3\right]$$
$$+ \frac{\pi}{24C}\left[(A+1+C)^3 + (A-1-C)^3 + (-A+1-C)^3 + (-A-1+C)^3\right]$$
$$+ \eta_1(B,C) \tag{3.3.55}$$

$$= -\frac{\pi}{24BC}[6A(B+C)^2 - 6A(B-C)^2] + \frac{\pi}{24C}[6A(1+C)^2 - 6A(1-C)^2] + \eta_1(B,C) \tag{3.3.56}$$

$$= -\frac{\pi A}{8BC}[4BC] + \frac{\pi A}{8C}[4C] + \eta_1(B,C) \tag{3.3.57}$$

$$= \eta_1(B,C) \tag{3.3.58}$$

implying $\eta_1(B,C) \equiv 0$.

As $A \to \infty$, Eq. (3.3.50) becomes

$$\lim_{A\to\infty} I_5 = \lim_{A\to\infty} -\frac{\pi}{96BC}\left[(A+B+C)^4 + (A-B-C)^4 - (-A+B-C)^4 - (-A-B+C)^4\right] + \frac{\pi}{96C}\left[(A+1+C)^4 + (A-1-C)^4 - (-A+1-C)^4 - (-A-1+C)^4\right] + \eta_2(B,C) \tag{3.3.59}$$

$$= \lim_{A\to\infty} -\frac{\pi}{96BC}\left[12A^2(B+C)^2 - 12A^2(B-C)^2 + 2(B+C)^4 - 2(B-C)^4\right] + \frac{\pi}{96C}\left[12A^2(1+C)^2 - 12A^2(1-C)^2 + 2(1+C)^4 - 2(1-C)^4\right] + \eta_2(B,C) \tag{3.3.60}$$

$$= \lim_{A\to\infty} -\frac{\pi}{96BC}\left[48A^2BC + 16BC + 16BC^3\right] + \frac{\pi}{BC}\left[48A^2C + 16C + 16C^3\right] + \eta_2(B,C) \tag{3.3.61}$$

$$= \frac{\pi}{6}(1-B^2) + \eta_2(B,C) \tag{3.3.62}$$

Comparing with Eq. (3.3.54), we deduce $\eta_2(B,C) \equiv 0$ which gives

$$I_5(A,B,C) = -\frac{1}{BC}Y_4(A,B,C) + \frac{1}{C}Y_4(A,1,C). \tag{3.3.63}$$

Hence,

$$T_3(A,B,C) = \frac{1}{BC}\frac{\partial}{\partial C}\frac{\partial}{\partial B}\left[-\frac{1}{BC}Y_4(A,B,C) + \frac{1}{C}Y_4(A,1,C)\right] \tag{3.3.64}$$

$$= -\frac{1}{BC}\frac{\partial^2}{\partial B\partial C}\left[\frac{Y_4(A,B,C)}{BC}\right] \tag{3.3.65}$$

3.3.4 Type IV Integrals

The fourth type of integral can be expressed,

$$T_4(A,B,C) = \frac{1}{ABC}\frac{\partial}{\partial A}\frac{\partial}{\partial B}\frac{\partial}{\partial C}\frac{1}{A}\int_{-\infty}^{\infty}\frac{\sin At \sin Bt \sin Ct}{BCt^7}dt \tag{3.3.66}$$

Using the same reasoning as for the third type of integral, while the integral above does not converge, we are able to introduce regularization terms into the integrand of Eq. (3.3.66)

as long as they are not functions of A, B and C simultaneously. Thus we can write

$$T_4(A,B,C) = \frac{1}{ABC}\frac{\partial}{\partial A}\frac{\partial}{\partial B}\frac{\partial}{\partial C}\frac{1}{A}\int_{-\infty}^{\infty}\frac{\sin At\sin Bt\sin Ct}{BCt^7} - \frac{\sin At\sin Bt\sin t}{Bt^7} - \frac{\sin At\sin t\sin Ct}{Ct^7} + \frac{\sin At\sin^2 t}{t^7}dt \tag{3.3.67}$$

$$= \frac{1}{ABC}\frac{\partial}{\partial A}\frac{\partial}{\partial B}\frac{\partial}{\partial C}\frac{1}{A}\int_{-\infty}^{\infty}\frac{\sin At}{t}\left[\frac{\sin Bt}{Bt^3} - \frac{\sin t}{t^3}\right]\left[\frac{\sin Ct}{ct^3} - \frac{\sin t}{t^3}\right]dt \tag{3.3.68}$$

Let

$$I_7(A,B,C) = \int_{-\infty}^{\infty}\frac{\sin At}{t}\left[\frac{\sin Bt}{Bt^3} - \frac{\sin t}{t^3}\right]\left[\frac{\sin Ct}{Ct^3} - \frac{\sin t}{t^3}\right]dt \tag{3.3.69}$$

which gives

$$\frac{\partial I_7}{\partial A} = \int_{-\infty}^{\infty}\cos At\left[\frac{\sin Bt}{Bt^3} - \frac{\sin t}{t^3}\right]\left[\frac{\sin Ct}{Ct^3} - \frac{\sin t}{t^3}\right]dt \tag{3.3.70}$$

and

$$\frac{\partial^2 I_7}{\partial A^2} = -\int_{-\infty}^{\infty}\cos At\left[\frac{\sin Bt}{Bt^3} - \frac{\sin t}{t^3}\right]\left[\frac{\sin Ct}{Ct^2} - \frac{\sin t}{t^2}\right]dt \tag{3.3.71}$$

$$= -\int_{-\infty}^{\infty}\frac{\sin At}{t}\left[\frac{\sin Bt}{Bt^3} - \frac{\sin t}{t^3}\right]\frac{\sin Ct}{Ct} - \frac{\sin At}{t}\left[\frac{\sin Bt}{Bt^3} - \frac{\sin t}{t^3}\right]\frac{\sin t}{t}dt \tag{3.3.72}$$

$$= -I_5(A,B,C) + I_5(A,B,1) \tag{3.3.73}$$

$$= \frac{1}{BC}Y_4(A,B,C) - \frac{1}{C}Y_4(A,1,C) - \frac{1}{B}Y_4(A,B,1) + Y_4(A,1,1). \tag{3.3.74}$$

Integrating, we find

$$\frac{\partial I_7}{\partial A} = \frac{1}{BC}Y_5(A,B,C) - \frac{1}{C}Y_5(A,1,C) - \frac{1}{B}Y_5(A,B,1) + Y_5(A,1,1) + \eta_1(B,C) \tag{3.3.75}$$

$$I_7(A,B,C) = \frac{1}{BC}Y_6(A,B,C) - \frac{1}{C}Y_6(A,1,C) - \frac{1}{B}Y_6(A,B,1) + Y_6(A,1,1) + A\eta_1(B,C) + \eta_2(B,C) \tag{3.3.76}$$

As usual, to determine η_1 and η_2, we take $\lim_{A\to\infty}$ of Eqs. (3.3.69 - 3.3.77). Since $\left[\frac{\sin Bt}{Bt^3} - \frac{\sin t}{t^3}\right]\left[\frac{\sin Ct}{Ct^3} - \frac{\sin t}{t^3}\right]$ is Riemann integrable, we can apply Lemmas 3.3.1 and 3.3.2 to obtain

$$\lim_{A\to\infty}\frac{\partial I_7}{\partial A} = \lim_{A\to\infty}\int_{-\infty}^{\infty}\cos At\left[\frac{\sin Bt}{Bt^3} - \frac{\sin t}{t^3}\right]\left[\frac{\sin Ct}{Ct^3} - \frac{\sin t}{t^3}\right]dt = 0 \tag{3.3.77}$$

and

$$\begin{aligned}\lim_{A\to\infty} I_7(A,B,C) &= \lim_{A\to\infty}\int_{-\infty}^{\infty}\frac{\sin At}{t}\left[\frac{\sin Bt}{Bt^3}-\frac{\sin t}{t^3}\right]\left[\frac{\sin Ct}{Ct^3}-\frac{\sin t}{t^3}\right]dt\\ &= \pi\lim_{t\to 0}\left[\frac{\sin Bt}{Bt^3}-\frac{\sin t}{t^3}\right]\left[\frac{\sin Ct}{Ct^3}-\frac{\sin t}{t^3}\right]\\ &= \frac{\pi}{36}(1-B^2)(1-C^2) \qquad (3.3.78)\end{aligned}$$

From Eq. (3.3.77), we also have

$$\begin{aligned}\lim_{A\to\infty}\frac{\partial I_7}{\partial A} &= \lim_{A\to\infty}\frac{1}{BC}Y_5(A,B,C)-\frac{1}{C}Y_5(A,1,C)-\frac{1}{B}Y_5(A,B,1)+Y_5(A,1,1)+\eta_1(B,C)\\ &= \lim_{A\to\infty}\frac{\pi}{480BC}\left[10A((B+C)^4-(B-C)^4)+20A^3((B+C)^2-(B-C)^2)\right]\\ &\quad-\frac{\pi}{480C}\left[10A((1+C)^4-(1-C)^4)+20A^3((1+C)^2-(1-C)^2)\right]\\ &\quad-\frac{\pi}{480B}\left[10A((B+1)^4-(B-1)^4)+20A^3((B+1)^2-(B-1)^2)\right]\\ &\quad-\frac{\pi}{480}\left[160A+80A^3\right]+\eta_1(B,C)\\ &= \lim_{A\to\infty}\frac{\pi}{480BC}\left[10A(8B^3C+8BC^3)+80A^3BC\right]-\frac{\pi}{480C}\left[10A(8C+8C^3)+80A^3C\right]\\ &\quad-\frac{\pi}{480B}\left[10A(8B^3+8B)+20A^3(80A^3B)\right]-\frac{\pi}{480}\left[160A+80A^3\right]+\eta_1(B,C)\\ &= \eta_1(B,C) \qquad (3.3.79)\end{aligned}$$

implying $\eta_1\equiv 0$. Similarly, in the limit of large A Eq. (3.3.76) becomes

$$\begin{aligned}&\lim_{A\to\infty} I_7(A,B,C) = \frac{1}{BC}Y_6(A,B,C)-\frac{1}{C}Y_6(A,1,C)-\frac{1}{B}Y_6(A,B,1)+Y_6(A,1,1)+\eta_2(B,C)\\ &= \lim_{A\to\infty}\frac{\pi}{2880BC}\left[2((B+C)^6-(B-C)^6)+30A^2((B+C)^4-(B-C)^4)+30A^4((B+C)^2-(B-C)^2)\right]\\ &\quad-\frac{\pi}{2880C}\left[2((1+C)^6-(1-C)^6)+30A^2((1+C)^4-(1-C)^4)+30A^4((1+C)^2-(1-C)^2)\right]\\ &\quad-\frac{\pi}{2880B}\left[2((B+1)^6-(B-1)^6)+30A^2((B+1)^4-(B-1)^4)+30A^4((B+1)^2-(B-1)^2)\right]\\ &\quad-\frac{\pi}{2880}\left[128+480A^2+120A^4)\right]+\eta_2(B,C)\\ &= \frac{\pi}{36}\left[B^2C^2-C^2-B^2+1\right]+\eta_2(B,C)\\ &= \frac{\pi}{36}(1-B^2)(1-C^2)+\eta_2(B,C)\end{aligned}$$

which, upon comparison with Eq. (3.3.78) we find $\eta_2 \equiv 0$. Therefore,

$$I_7(A,B,C) = \frac{1}{BC}Y_6(A,B,C) - \frac{1}{C}Y_6(A,1,C) - \frac{1}{B}Y_6(A,B,1) + Y_6(A,1,1) \tag{3.3.80}$$

and

$$\begin{aligned} T_4(A,B,C) &= \frac{1}{ABC}\frac{\partial}{\partial A}\frac{\partial}{\partial B}\frac{\partial}{\partial C}\left[\frac{1}{ABC}Y_6(A,B,C) - \frac{1}{AC}Y_6(A,1,C) - \frac{1}{AB}Y_6(A,B,1) + \frac{1}{A}Y_6(A,1,1)\right] \\ &= \frac{1}{ABC}\frac{\partial}{\partial A}\frac{\partial}{\partial B}\frac{\partial}{\partial C}\frac{Y_6(A,B,C)}{ABC} \end{aligned} \tag{3.3.81}$$

3.3.5 Evaluation of the coefficient

In summary, we have found

$$\int_{-\infty}^{\infty} \frac{\sin At \sin Bt \sin Ct}{t} dt = -Y_0(A,B,C) \tag{3.3.82}$$

$$\int_{-\infty}^{\infty} \sin At \sin Bt\, g(Ct) dt = \frac{1}{C}\frac{\partial}{\partial C}\frac{Y_2(A,B,C)}{C} \tag{3.3.83}$$

$$\int_{-\infty}^{\infty} \sin At\, g(Bt) g(Ct) t dt = -\frac{1}{BC}\frac{\partial^2}{\partial B \partial C}\frac{Y_4(A,B,C)}{BC} \tag{3.3.84}$$

$$\int_{-\infty}^{\infty} \frac{\sin At \sin Bt \sin Ct}{t} dt = \frac{1}{ABC}\frac{\partial^3}{\partial A \partial B \partial C} Y_6(A,B,C)ABC \tag{3.3.85}$$

where

$$\begin{aligned} Y_n(A,B,C) = \frac{\pi}{4n!}[&(A+B+C)^{n-1}|A+B+C| + (A-B-C)^{n-1}|A-B-C| + \\ &(-1)^n(-A+B-C)^{n-1}|-A+B-C| + (-1)^n(-A-B+C)^{n-1}|-A-B+C|] \end{aligned} \tag{3.3.86}$$

and

$$g(x) = \frac{\cos x}{x^2} - \frac{\sin x}{x^3}. \tag{3.3.87}$$

Collecting these results, we can write Eq. (3.3.8) as

$$\begin{aligned}
&\int_0^\infty \left[\frac{\sin At}{2A\tau_A t} + g(At)\right]\left[\frac{\sin Bt}{2B\tau_B t} + g(Bt)\right]\left[\frac{\sin Ct}{2C\tau_C t} + g(Ct)\right] t^2 dt \\
&\quad = \frac{1}{16ABC}\Big[- \frac{Y_0(A,B,C)}{\tau_A\tau_B\tau_C} + \frac{2}{\tau_A\tau_B}\frac{\partial}{\partial C}\frac{Y_2(A,B,C)}{C} + \frac{2}{\tau_A\tau_C}\frac{\partial}{\partial B}\frac{Y_2(A,C,B)}{B} \\
&\quad + \frac{2}{\tau_B\tau_C}\frac{\partial}{\partial A}\frac{Y_2(B,C,A)}{A} - \frac{4}{\tau_A}\frac{\partial^2}{\partial B\partial C}\frac{Y_4(A,B,C)}{BC} - \frac{4}{\tau_B}\frac{\partial^2}{\partial A\partial C}\frac{Y_4(B,A,C)}{AC} \\
&\quad - \frac{4}{\tau_C}\frac{\partial^2}{\partial A\partial B}\frac{Y_4(C,A,B)}{AB} + 8\frac{\partial^3}{\partial A\partial B\partial C}\frac{Y_6(A,B,C)}{ABC}\Big].
\end{aligned} \tag{3.3.88}$$

Hence, for $A = d_{ij}, B = d_{jk}$ and $C = d_{ik}$, the third virial coefficient, C_{ijk}, can be expressed as

$$\begin{aligned}
C_{ijk}(T) = -\frac{2\pi}{3}d_{ij}^2 d_{jk}^2 d_{ik}^2\Big[&- \frac{Y_0(d_{ij},d_{jk},d_{ik})}{\tau_{ij}\tau_{jk}\tau_{ik}} + \frac{2}{\tau_{ij}\tau_{jk}}\frac{\partial}{\partial d_{ik}}\frac{Y_2(d_{ij},d_{jk},d_{ik})}{d_{ik}} \\
&+ \frac{2}{\tau_{ij}\tau_{ik}}\frac{\partial}{\partial d_{jk}}\frac{Y_2(d_{ij},d_{ik},d_{jk})}{d_{jk}} + \frac{2}{\tau_{jk}\tau_{ik}}\frac{\partial}{\partial d_{ij}}\frac{Y_2(d_{jk},d_{ik},d_{ij})}{d_{ij}} \\
&- \frac{4}{\tau_{ij}}\frac{\partial^2}{\partial d_{jk}\partial d_{ik}}\frac{Y_4(d_{ij},d_{jk},d_{ik})}{d_{jk}d_{ik}} - \frac{4}{\tau_{jk}}\frac{\partial^2}{\partial d_{ij}\partial d_{ik}}\frac{Y_4(d_{jk},d_{ij},d_{ik})}{d_{ij}d_{ik}} \\
&- \frac{4}{\tau_{ik}}\frac{\partial^2}{\partial d_{ij}\partial d_{jk}}\frac{Y_4(d_{ik},d_{ij},d_{jk})}{d_{ij}d_{jk}} + 8\frac{\partial^3}{\partial d_{ij}\partial d_{jk}\partial d_{ik}}\frac{Y_6(d_{ij},d_{jk},d_{ik})}{d_{ij}d_{jk}d_{ik}}\Big]
\end{aligned} \tag{3.3.89}$$

We can simplify this further if we notice that all instances of Y_n appearing in Eq. (3.3.89) contain *even* values of n. If n is even then,

$$\begin{aligned}
Y_n^{even}(A,B,C) = \frac{\pi}{4n!}[&(A+B+C)^n + (A-B-C)^{n-1}|A-B-C| + \\
&(-A+B-C)^{n-1}|-A+B-C| + (-A-B+C)^{n-1}|-A-B+C|]
\end{aligned} \tag{3.3.90}$$

which is now a symmetric function of A, B and C. Additionally, when closest center-to-center distances $d_{ij} = \frac{1}{2}(d_{ii} + d_{jj})$, $d_{jk} = \frac{1}{2}(d_{jj} + d_{kk})$ and $d_{ik} = \frac{1}{2}(d_{ii} + d_{kk})$ are substituted for A, B and C we see that

- $A - B - C = -d_{kk} < 0$
- $-A + B - C = -d_{ii} < 0$
- $-A - B + C = -d_{jj} < 0$

Thus the quantities appearing in the absolute value signs in Eq. (3.3.90) are always *strictly*

negative for physical values of A, B, C. By the symmetry of Y for n even, we find

$$Y_n^{even}(d_{ij}, d_{jk}, d_{ik}) = \frac{\pi}{4n!}[(d_{ii} + d_{jj} + d_{kk})^n - (d_{ii})^n - (d_{jj})^n - (d_{kk})^n] \tag{3.3.91}$$

which is now simply a polynomial in the particle diameters. Substituting Eq. (3.3.91) into Eq. (3.3.89) and simplifying we arrive at the closed form expression:

$$\begin{aligned} C_{ijk}(T) = \frac{\pi^2}{54\tau_{ij}\tau_{jk}\tau_{ik}}\Big[& d_{ij}^6(\tau_{ij}-3)\tau_{jk}\tau_{ik} - 9d_{ij}^4(\tau_{ij}-2)(d_{ik}^2(\tau_{ik}-1)\tau_{jk} + d_{jk}^2\tau_{ik}(\tau_{jk}-1)) \\ & + 4d_{ij}^3(2\tau_{ij}-3)(d_{ik}^3(2\tau_{ik}-3)\tau_{jk} + d_{jk}^3\tau_{ik}(2\tau_{jk}-3)) \\ & - 9d_{ij}^2(\tau_{ij}-1)(d_{ik}^4(\tau_{ik}-2)\tau_{jk} - 2d_{ik}^2d_{jk}^2(\tau_{ik}-1)(\tau_{jk}-1) + d_{jk}^4\tau_{ik}(\tau_{jk}-2)) \\ & + \tau_{ij}(d_{ik}-d_{jk})^2(d_{ik}^4(\tau_{ik}-3)\tau_{jk} + 2d_{ik}^3d_{jk}(\tau_{ik}-3)\tau_{jk} + 3d_{ik}^2d_{jk}^2(\tau_{ik}(3-2\tau_{jk}) \\ & + 3(\tau_{jk}-2)) + 2d_{ik}d_{jk}^3\tau_{ik}(\tau_{jk}-3) + d_{jk}^4\tau_{ik}(\tau_{jk}-3))\Big]. \end{aligned} \tag{3.3.92}$$

We know that in the absence of adhesion, the Barboy-Baxter model should reduce to a hard sphere mixture. Therefore, we can compare our expression for C_{ijk} as $\{\tau_{ij}\} \to \infty$, to expressions for the pure and mixed hard-sphere third virial coefficients which are well documented. In the limit $\{\tau_{ij}\} \to \infty$, we find

$$\begin{aligned} C_{ijk}^{HS} = \frac{\pi^2}{54}\Big[& d_{ij}^6 + d_{jk}^6 + d_{ik}^6 + 18d_{ij}^2d_{jk}^2d_{ik}^2 + 16(d_{ij}^3d_{ik}^3 + d_{ij}^3d_{jk}^3 + d_{ik}^3d_{jk}^3) \\ & - 9d_{ij}^4(d_{jk}^2 + d_{ik}^2) - 9d_{jk}^4(d_{ij}^2 + d_{ik}^2) - 9d_{ik}^4(d_{ij}^2 + d_{jk}^2)\Big] \end{aligned} \tag{3.3.93}$$

which agrees with the hard sphere expressions found in [26] and [27].

Now that we have expressions for B_{ij} and C_{ijk}, we may use a truncated form of the virial expansion of the Gibbs free energy given in Eq. (3.1.3) directly in the light scattering equation (Eq. (2.3.1)). This will provide additional insight into the molecular basis of lens transparency, by allowing us to view light scattering intensity as an explicit function of concentration.

Chapter 4

Conclusion and Future Work

We have shown that the Baxter-Barboy sticky sphere model can semi-quantitatively reproduce light scattering intensities for aqueous α/γ_B mixtures at concentrations found in the living lens. This serves as an important step forward in understanding the molecular mechanism of lens transparency and cataract. Future work includes extending the Baxter-Barboy model to quaternary mixtures of α, β and γ-crystallins in buffer for comparison to upcoming light scattering experiments. Using the general root finding method described in Section 2.2.2, this extension should be straightforward. With additional data, one can use the model, and virial coefficients, to estimate crystallin interaction strengths and their dependence on temperature. Furthermore, one can compute light scattering intensities through the virial expansion of the Gibbs free energy (Eq. (3.1.3)) using the analytic expressions for B_{ij} and C_{ijk} derived in this thesis. Since the virial expansion only depends on the form of the intermolecular potential and not on the closure used to solve for the correlation functions, this can provide added insight to the mechanism of lens transparency.

Bibliography

[1] G.M. Thurston. Liquid-liquid phase separation and static light scattering of concentrated ternary mixtures of bovine Alpha and GammaB crystallins. *Journal of Chemical Physics*, 124:134909, 2006.

[2] A. Stradner, G. Foffi, N. Dorsaz, G. Thurston, and P. Schurtenberger. New insight into cataract formation: Enhanced stability through mutual attraction. *Physical Review Letters*, 99(19), November 2007.

[3] M. Delaye and A. Tardieu. Short-range order of crystallin proteins accounts for eye lens transparency. *Nature*, 302(5907):415–417, 1983.

[4] GB Benedek. Cataract as a protein condensation disease: the proctor lecture. *Investigative ophthalmology & visual science*, 38(10), 09 1997.

[5] S. Finet and A. Tardieu. γ-crystallin interaction forces studied by small angle x-ray scattering and numerical simulations. *Journal of Crystal Growth*, 232(1-4):40–49, 2001.

[6] BM Fine, A Lomakin, OO Ogun, and GB Benedek. Static structure factor and collective diffusion of globular proteins in concentrated aqueous solution. *Journal of Chemical Physics*, 104(1):326–335, JAN 1 1996.

[7] P.R. Banerjee, A. Pande, J. Patrosz, G.M. Thurston, and J. Pande. Cataract-associated mutant E107A of human gamma D-crystallin shows increased attraction to alpha-crystallin and enhanced light scattering. *PNAS(USA)*, 108(2):574–579, 2011.

[8] N. Dorsaz, G.M. Thurston, A. Stradner, P. Schurtenberger, and G. Foffi. Colloidal characterization and thermodynamical stability of binary eye lens proteins mixtures. *J. Phys. Chem. B.*, 113:1693–1709, 2009.

[9] N. Dorsaz, G.M. Thurston, A. Stradner, P. Schurtenberger, and G. Foffi. Phase separation in binary eye lens protein mixtures. *Soft Matter*, 7(5):1763–1776, 2011.

[10] RJ Baxter. Ornstein-Zernike Relation and Percus-Yevick Approximation for Fluid Mixtures. *Journal of Chemical Physics*, 52(9):4559–&, 1970.

[11] B Barboy and R Tenne. Distribution functions and equations of state of sticky hard-sphere fluids in the Percus-Yevick approximation. *Chemical Physics*, 38(3):369–387, 1979.

[12] RJ Baxter. Percus-Yevick Equation for Hard Spheres with Surface Adhesion. *Journal of Chemical Physics*, 49(6):2770–&, 1968.

[13] B. Barboy. Solution of compressibility equation of adhesive hard-sphere model for mixtures. *Chemical Physics*, 11(3):357–371, 1975.

[14] C.N. Lahnovych. Analysis and computation of a quadratic matrix polynomial with schur-products and applications to the barboy-tenne model. Master's thesis, Rochester Institute of Technology, 2010.

[15] A.J. Sommese and C.W. Wampler. *The numerical solution of systems of polynomials arising in engineering and science*. World Scientific, 2005.

[16] A. Dickenstein and I.Z. Emiris. *Solving polynomial equations: foundations, algorithms, and applications*. Algorithms and computation in mathematics. Springer, 2005.

[17] J.G. Kirkwood and R.J. Goldberg. Light scattering arising from composition fluctuations in multi-component systems. *J. Chem. Phys.*, 18:54–57, 1950.

[18] T.L. Hill. *Statistical Mechanics*. Dover, 1987.

[19] D.S. Ross, G.M. Thurston, and C.V. Lutzer. On a partial differential equation method for determining the free energies and coexisting phase compositions of ternary mixtures from light scattering data. *J. Chem. Physics*, 129(6), 2008.

[20] J. Bloustine, T. Virmani, G.M. Thurston, and S. Fraden. Light scattering and phase behavior of lysozyme-poly(ethylene glycol) mixtures. *Physical Review Letters*, 96:087803, 2006.

[21] D.A. McQuarrie. *Statistical Mechanics*. Harper and Row, 1976.

[22] John S. Rowlinson and Donald A. McQuarrie. The third virial coefficient of hard discs of different sizes. *Molecular Physics*, 61(2):525–528, 1987.

[23] A. Vretblad. *Fourier analysis and its applications*. Graduate texts in mathematics. Springer, 2003.

[24] E.A. Kraut. *Fundamentals of mathematical physics*. McGraw-Hill series in fundamentals of physics. McGraw-Hill, 1967.

[25] F.B. Hildebrand. *Methods of applied mathematics*. Dover books on advanced mathematics. Dover Publications, 1965.

[26] E.A. Mason and T.H.J.A. Spurling. *The Virial Equation of State, By E.A. Mason and T.H. Spurling*. International Encyclopedia of Physical Chemistry and Chemical Physics. (Oxford) Topic 10: the Fluid State, V.2. Pergamon Press, 1969.

[27] J.O. Hirschfelder, C.F. Curtiss, R.B. Bird, and University of Wisconsin. Theoretical Chemistry Laboratory. *Molecular theory of gases and liquids*. Structure of matter series. Wiley, 1954.